Macromolecular Rapid Communications
www.mrc-journal.de

Check for updates

Advances in the Stimuli-Responsive Injectable Hydrogel for Controlled Release of Drugs

*Chunxiang Mo, Rui Luo, and Yuping Chen**

The stimuli-responsiveness of injectable hydrogel has been drastically developed for the controlled release of drugs and has achieved encouraging curative effects in a variety of diseases including wounds, cardiovascular diseases, and tumors. The gelation, swelling, and degradation of such hydrogels respond to endogenous biochemical factors (such as pH, reactive oxygen species, glutathione, enzymes, glucose) and/or to exogenous physical stimulations (like light, magnetism, electricity, and ultrasound), thereby accurately releasing loaded drugs in response to specifically pathological status and as desired for treatment plan, and thus improving therapeutic efficacy effectively. This paper gives a detailed introduction of recent progresses in responsive injectable hydrogels and focuses on the design strategy of various stimuli-sensitivities and their resultant alteration of gel dissociation and drug liberation behavior. Their application in disease treatment is also discussed.

1. Introduction

Injectable hydrogels are a special class of hydrogels that are injected into the target site and gel in situ. Their gelling molecules are often non-crosslinked and soluble before syringe injection, but rapidly react and entangle with each other to finish a sol–gel transition upon being mixed and entering into the body. Some hydrogels solidify in vitro, fluidize due to the mechanical shearing from syringe needle, and resume back to gel status after injection, as shown in the case of so-called self-healing hydrogel.[1,2] Until 2019, 28 injectable hydrogels have been given official admits for clinical uses and another 31 products have been approved by the FDA(Food and Drug Administration)and/or EMA (European Medicines Agency) for clinical trials, mainly in cardiovascular disease, cancer, bone damage, and cosmetics.[3] Especially encouraging is that UC San Diego News Center reported the successful injection of VentriGel via a catheter into patients with a heart attack 2–36 months ago and the improvement of their heart damage in a phase I trial. Its phase II trial is currently ongoing.

C. Mo, R. Luo, Y. Chen
Institute of Pharmacy & Pharmacology
School of Pharmaceutical Science
University of South China
Hengyang 410001, China
E-mail: yupingc@usc.edu.cn

The ORCID identification number(s) for the author(s) of this article can be found under https://doi.org/10.1002/marc.202200007

DOI: 10.1002/marc.202200007

Because of their injectability, the three dimensional (3D) net-work structure, and biocompatible physiochemical features, injectable hydrogels are widely exploited as a local drug reservoir to achieve a controlled drug release, avoid first-pass effect, and enhance patient compliance. Compared to other common long-acting injectable preparations such as polymer-based microspheres, oil-based injectable solutions, and injectable-drug suspensions,[4] injectable hydrogels possess unique advantages and thus are able to accomplish certain special applications in the treatment of diseases such as tumors, wounds, and CVDs (Cardiovascular Disease). They take shape at lesion site into a gel, which provides not only mechanical support to the tissues but also protection for loaded drugs or therapeutic cells from extrusion. Their hydrophilic gel network also allows cells to live in an extracellular matrix (ECM)-mimicking ambient and places the liberation of drug cargos under multiple levels of controls from porosity, pore size, to drug hydrodynamics.[5,6] Microspheres are another major type of injectable drug delivery systems. Their outstanding dispersity and diffusivity ensure a nice injectability and uniformity in drug release, so their performance is especially superior in local treatment on solid tumors and wounds.[7–11] Comparably, though still struggling with challenges such as drug burst and potential mechanical injury to tissue, injectable hydrogels are more elastic,[12] plastic,[13] tissue-retentive,[7] and ECM-like, so are obviously more adjustable to coat over wounds with various shapes, more applicable for tumors growing in different sites, and more suitable for contractile hearts.[14]

The drug release rate and dose are key factors for the success of therapeutic injectable hydrogel, which are primarily governed in diffusion-, swelling-, and chemical degradation-controlling ways.[15–17] Ordinary hydrogels can release cargos slowly but not in a controlled fashion. In contrast, the responsive injectable hydrogels significantly alter their 3D network structure, swelling behavior, permeation property, or mechanical strength when exposed to corresponding stimuli, and thus modify their drug release behavior.[18] In fact, pathological microenvironment dynamics can offer multiple biochemical stimuli suitable for gel responsiveness construction, for example, low pH in wounds,[19] rising glutathione (GSH)[20] and reactive oxygen species (ROS) in cancer,[21] abundant matrix metalloproteinase (MMP) in infarcted heart tissue,[22] and high blood sugar in diabetes patients,[23] and designing the sensitivity to these stimuli

 © 2022 Wiley-VCH GmbH

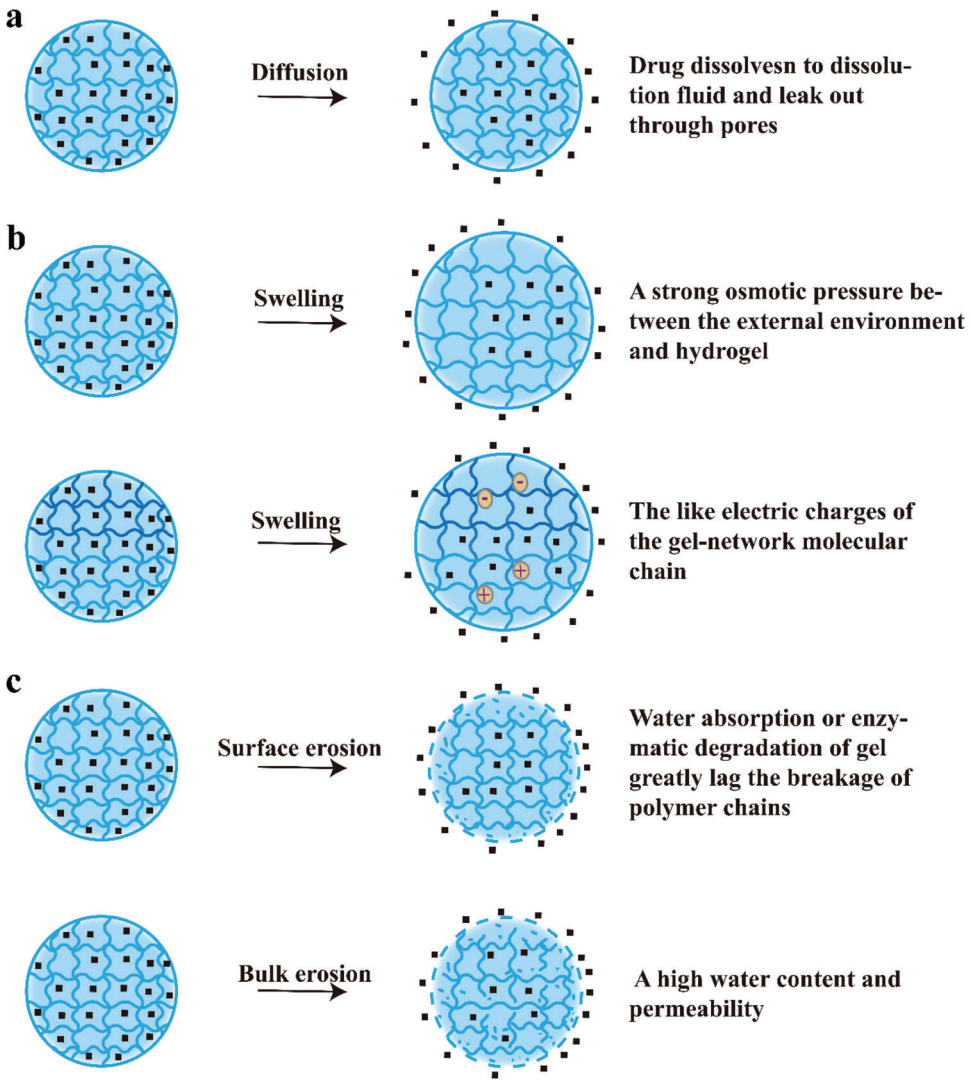

Figure 1. Illustration of three main mechanisms for the sustained drug release of hydrogels. a) Drug diffusion, b) swelling, and c) chemical erosion.

into injectable hydrogel has achieved a controlled drug release to match disease severity. On another side, the reactivity to more controllable physical stimuli such as light, magnetism, electricity, and ultrasound has also been introduced into hydrogel and the on-off pulsed drug-delivery system obtained.[24] Such systems can even program their drug emancipation as needed, for example, continuously release a certain amount in a short time after a predetermined release period according to the circadian rhythm of disease state.[25]

Here, we summarize recent progresses in this exciting research field, focus on the design of stimuli reactivity and its regulation of gel's drug release conduct, and discuss how environmental sensitivity of injectable hydrogels affects their drug carry and liberation and their applicable disease therapy.

2. Drug Release of Injectable Hydrogel

As aforementioned, the drug release from injectable hydrogels is mainly determined by drug diffusion, gel swelling/degradation, and chemical condition. Molecule diffusion is the most widely applicable mechanism (**Figure 1**a). It follows Fick's law of diffusion,[17] and is influenced by porosity and pore size in hydrogel matrix that can be adjusted by several parameters such as the cross-linking degree and chemical structure of composing monomers in gel body.[26,27]

Hydrogel inflates under osmotic swelling force, driving water entry into hydrophilic network and altering gel molecule interplay and thus hydrogel structure (Figure 1b). In neutral networks, the initially high concentration of polymers easily creates a strong osmotic pressure between solvent and hydrogel, which forces solvent molecules into gel network and increases gel volume. As for a polyelectrolyte gel, its free ions generate an additional ion concentration difference between solvent and gel body to attract solvent into the gel, providing more osmotic pressure. Besides, the like electric charges of the gel-network backbone repel each other, compelling polymer chains to stretch, therefore dilating the gel.[28,29] The molecular weight and cross-linking density of gelation polymers also affect the swelling rate of hydrogels.

© 2022 Wiley-VCH GmbH

Table 1. pH-Responsive injectable hydrogel.

Strategy	Responsive linkage	Gelation molecules	pH	Drug	Disease	Ref.
Acid-sensitive covalent bonds	Imine bond	QCS and PF127-CHO	7.4–6.0	Curcumin	Wounds	[62]
		GC and OHC-PEO-PPO-PEO-CHO	7.4 and 6.8	DOX and paclitaxel	Melanoma cancer	[63]
		PFA and PPLL	7.4–6.0	Metformin and 5-fluorouracil	Colon carcinoma	[64]
		CEC and PEGDA	7.4–4.0	DOX	HCC	[33]
	Hydrazone bond	PAHy and GPAAld	7.4 and 5.0	DOX	HCC	[65]
Cationic groups	Tertiary amine group	PBAEs	7.4 and 5.0	Methylene blue	–	[66]
		PEG-PACU	7.4–6.0	Growth hormone	–	[67]
	Sulfonamide group	PEG and PSMEU	11.0–6.8	Lysozyme	Wounds	[68]
Anionic groups	Carboxyl group	PAA and NIPAAM	7.4–5.0	VEGF	–	[69]
		p[NIPAAm-*co*-PAA-*co*-BA]	7.4 and 6.8	Fibroblast growth factor	IM	[56]
		PGA, GPTMS, and TEOS	7.4 and 1.2	DOX and tetracycline	–	[70]
Electro-static interaction		Gelatin and laponite	9.18	Rhodamine	–	[60]
Coordinate bond	Coordinate bond	4PEG-Phis and Ni^{2+} ions,	7.4	–	–	[61]
		HPCH/TA/Fe^{3+}	9.0–3.0	Tannic acid	Wounds	[71]

QCS, quaternized chitosan; PF127-CHO, the benzaldehyde-terminated Pluronic®F127; DOX, doxorubicin; GC, glycol chitosan benzaldehyde; PEO, poly(ethylene glycol); PPO, poly(propylene glycol); PFA, aldehyde-functionalized four-arm polyethylene glycol; PPLL, 4-arm poly(ethylene glycol)-*b*-poly(L-lysine); CEC, N-carboxyethyl chitosan; PEGDA, dibenzaldehyde-terminated poly(ethylene glycol); PAHy and GPAAld, poly (α,β-aspartic acid) derivatives; PBAEs, poly(β-amino ester); PEG, poly(ethylene glycol); PACU, poly(amino carbonate urethane); PSMEU, poly(sulfamethazine ester urethane); PAA, propylacrylic acid; NIPAAM, N-isopropylacrylamide; VEGF, vascular endothelial growth factor; p[NIPAAm-*co*-PAA-*co*-BA], poly(N-isopropylacrylamide-*co*-propylacrylic acid-*co*-butyl acrylate); PGA, poly (γ-glutamic acid); GPTMS, 3-glycidoxypropyl trimethoxysilane; TEOS, hydrolyzed tetraethylorthosilicate; 4PEG-Phis, poly(ethylene glycol)-*b*-polyhistidine; HPCH/TA/Fe^{3+}, hydroxypropyl chitin/tannic acid/ferric ion; HCC, hepatocellular carcinoma; IM, infarcted myocardium.

The larger the constituting polymers, the denser the cross-linking of the 3D hydrogel network, and the lower the swelling rate of hydrogel.[27,30]

Hydrogel undergoes chemical degradation as shown by bulk erosion and surface erosion, both contributing to the controlled drug release by hydrogel in different ways (Figure 1c). Hydrogel has a high water content and permeability, enabling the chain scission of polymers to occur in entire gel matrix and bulk erosion. Surface erosion occurs when water absorption or enzymatic degradation of gel greatly lag the breakage of polymer chains. Obviously, erosion changes the volume and shape of 3D gel network structure and the release of loaded drugs.[31] Generally, cross-linking density and chemical stimulation are two major factors affecting the chemically controlled drug release. The denser the molecular cross-linking, the slower the degradation, thereby slowing down the drug leaving from the gel in a chemically controlled way.[32]

In sum, gel structure matters the most among many factors influencing drug whereabouts, and therefore has been the major target for various stimuli to carry out desirable liberation of gel payload. Usually, stimuli modify gel structure by changing pore size, gel network expansion, gel–sol phase transition, covalent bonds between the polymers, non-covalent linkages in gel network, and so on.[33–36]

3. Stimuli-Responsive Injectable Hydrogel

Presently, the stimuli controlling the release of injectable hydrogel-laden drugs include the chemical/biochemical and physical.[18] The former comes from lesional site and changes with disease development, consisting of pH, ROS, GSH, enzymes, and glucose.[37] The latter are types of physical stimuli manipulated exogenously, including light, magnetism, electricity, and ultrasound.[24] The responsiveness to these two kinds of stimulations often exists simultaneously in injectable hydrogels.

3.1. Injectable Hydrogel Reactive to Endogenous Chemical/Biochemical Stimuli

Abnormal metabolism of diseased cells/tissues remodels their microenvironment and alters the levels of pH, ROS, GSH, enzymes, and glucose,[38] and the degree of change closely correlates to the extent of disease progression. So the reactivity to such disease-related endogenous signals has been first considered into injectable hydrogel.

3.1.1. pH-Responsive Injectable Hydrogels

***The Strategy to Introduce pH-Sensitivity into Injectable Hydrogel*:** **Table 1** presents common strategies for the preparation of pH-responsive injectable hydrogel: 1) cross-linking gel molecules via pH-sensitive covalent bonds, such as imine bonds[39] and acyl hydrazone bonds;[40] 2) constituting gel with polymers with abundant acidic (such as sulfonic acid and carboxyl) or basic (such as amino) groups;[38,41,42] 3) gelling upon electrostatic interaction[43] or coordination bond.[44]

The representatives of acid-sensitive covalent bonds are the Schiff base reaction–based imine bonds and acylhydrazone

© 2022 Wiley-VCH GmbH

bonds, where nucleophilic N atom of amino group attacks aldehyde/ketone group to generate a linkage of chemical bond, $R_1N = CR_2R_3$, where R_1, R_2, and R_3 can be alkyl, aryl, heteroaryl, hydrogen, etc.[45,46] Such bonds form rapidly and reversibly under physiological conditions, but are easily broken by mechanical force such as syringe needle shearing or become instable in an acidic environment, generating the self-healing behavior and injectability for the hydrogel containing imine or hydrazone bonds.[47,48] Acylhydrazone bond is more stable compared with imine bond, which is due to the mesomeric effect during hydrolysis that reduces the electrophilicity of the imine bond of acylhydrazone bond to a certain extent, thereby slowing down the hydrolysis and transamination of acylhydrazone bond.[49]

Gel's pH-sensitivity can also be achieved by conjugating the main chains of gelling polymers with abundant ionizable pendant groups, like amino, sulfonic, or carboxyl groups.[37] The ionization of such groups charges those gelling polymers under specified pH conditions, prompting their water absorption and electrostatic repulsion and thus swelling hydrogel.[50,51] Cationic injectable hydrogel is often prepared by amino-rich polymeric materials, like poly(*β*-amino ester) (PAE),[52] poly(amino urethane) (PAU),[53] poly(amino ureaurethane) (PAUU),[54] and other polyurethane derivatives. In contrast, the dissolution behavior of anionic injectable hydrogels opposes that of the cationic ones. Specifically, a high pH ionizes anionic groups of gelling polymers, which increases more counter ions in polymer network, augments osmotic pressure difference between the internal and external environment of the polymers, and prompts their electrostatic repulsion and gel swelling.[55] So far, the polymers with abundant carboxyl groups, such as propylacrylic acid (PAA),[56] carboxymethyl chitosan,[57] and polyamino-acid,[58] have been applied to construct anionic injectable hydrogels and establish a pH-sensitive drug release.

The force to drive gelation also comes from moderate intramolecular interactions among gel molecules, for example coordination bonds, ionic interactions, host–guest chemistry, hydrogen bonds, hydrophobic interactions, and *π*–*π* stacking interactions. These weak bonds possess unique features like reversible bonding, shear-thinning and stimuli responsiveness,[59] thus underpinning the injectability and controlled drug release of the gels that are based on such interactions. Obviously, the stability of these fragile linkages is also under the control of pH because its fluctuation would vacillate the established balance between electrostatic attraction and repulsion[60] or disrupt the coordination bonds supporting hydrogel network structure.[61]

The Application of pH-Sensitivity in Biomedical Injectable Hydrogels: The pH varies with physio- and pathological conditions, being 5.4 to 7.4 at wounds, 6.5 to 7.2 in tumor cells, 7.34 to 7.45 in blood, and 4.8 to 8.2 at the upper small intestine.[37] The pH-responsive injectable hydrogels have been widely applied in local therapeutical treatment on these illnesses. Qu et al.[62] prepared a pH-responsive hydrogel for wounds curation, the QCS/PF hydrogels. In this gel, the amino groups of the quaternized chitosan (QCS) formed imine bonds with the aldehyde groups of the benzaldehyde-terminated Pluronic®F127 (PF127-CHO) via the Schiff base reaction (**Figure 2**a). No blockage occurred when squeezing the obtained hydrogel through a 26-gauge needle, suggesting its excellent injectability. The QCS/PF hydrogel was used to load curcumin and then subjected to drug release assay. As

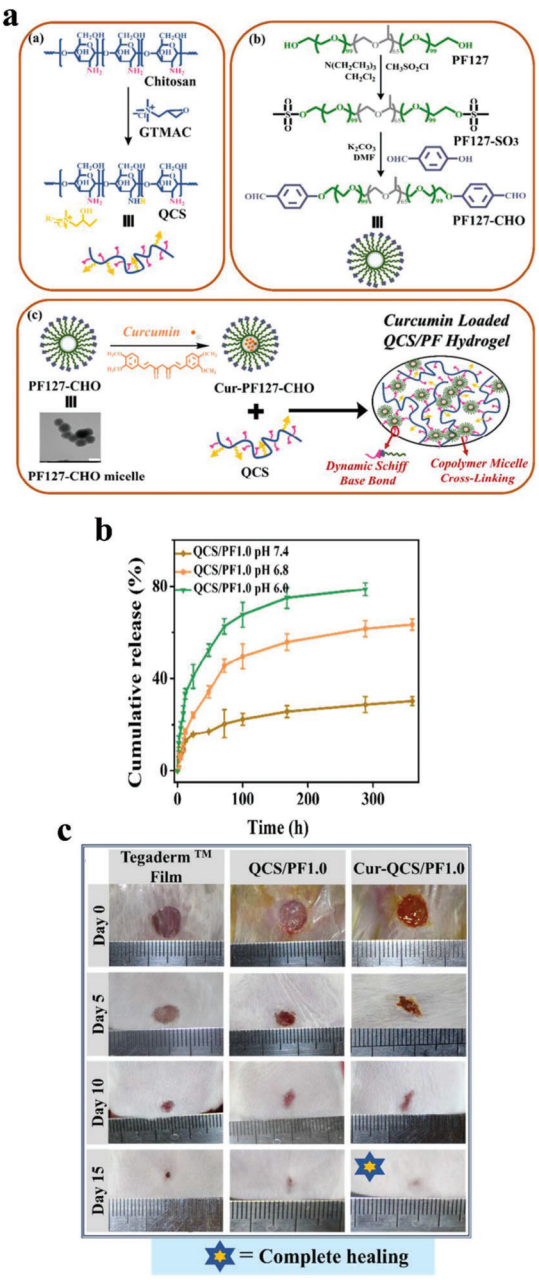

Figure 2. a) Schematic representation of Cur-QCS/PF hydrogel synthesis. b) In vitro release kinetics of curcumin from the hydrogels in PBS at different pH values. c) Photographs of wounds. Reproduced with permission.[62] Copyright 2018, Elsevier.

expected, the resultant Cur-QCS/PF released approximately 78% curcumin after staying in PBS for 288 h at pH 6.0 whereas the release was lowered to 61% and 28% at pH 6.8 and 7.4, respectively (Figure 2b), showing its good acid-reactivity. After being injected into wounded animals, the Cur-QCS/PF1.0 hydrogel (-CHO/-NH2 ratio = 1.0) generated the largest wound contraction area (72%) compared to commercial films and the drug free hydrogel, indicating that it achieved a relatively better promotion of wound healing (Figure 2c). Clearly, these results demonstrated that the imine bond-based Cur-QCS/PF hydrogels could really

© 2022 Wiley-VCH GmbH

propel a pH-responsive drug release to accelerate wound healing. Similarly, the acylhydrazone bond-based acid-sensitive gel has also been injected into acidic wound microenvironment or glycolytic tumor surroundings to fulfill an acid-promoted drug release and better treatment efficacy.[33,65,72,73] Overall, the Schiff base reaction takes place at a fast rate in aqueous solutions under physiological conditions without toxic by-products, ensuring attractive biosafety and applicability for the Schiff base reaction-dependent pH-responsive injectable hydrogel in vivo.[73–75]

Bingol et al. took use of the second strategy to yield pH responsiveness for injectable hydrogel.[66] They had cystamine mixed and reacted with poly(ethylene glycol) diacrylate (PEGDA) or PEGDA/1,6-hexanediol diacrylate (HDDA) via aza-Michael reaction to fabricate a temperature and acid double responsive poly(*β*-amino ester) (PBAE) injectable hydrogel. The gel precursor solution remained liquid state before injection and gelled in situ after entering into a warmer internal environment. It was seen that three PBAE hydrogels prepared with the increasing ratios of PEGDA:HDDA and accordingly named H1, H2, and H3, disintegrated under a low pH condition with a varying acid sensitivity. H1 gel completely degraded within 24 h no matter acidic (pH 5) or neutral (pH 7.4) soaking buffer used, being too susceptible to acidic stimulation to be further analyzed. H2 gel had a slower and clearly pH-dependent degradation. It only lost 15% weight after staying in neutral buffer for 24 h and spent another 120 h more to be totally dissociated, whereas its weight loss at 24 h rose to 25% in acidic soaking solution and its degradation was complete at 120 h. Consistently, the lowest degradation was seen in H3 gel. Less than 5% of H3 gel was lost after 1 day staying in two buffers, and soaking gel in acidic buffer for 10 days only resulted in 28% weight loss. However, pH responsiveness remained for H3 gel since its weight loss rose from 28% to 55% after 10 days' immersion in sour solution. Methylene blue (MB), a model drug and photosensitizer for photodynamic therapy (PDT) was then loaded into the PBAE hydrogel during gel preparation. Such a prepared MB-PBAE gel freed MB into acidic environments faster than into neutral ones, exhibiting a pH-dependent release behavior.

Similarly, an alkali-responsive hydrogel was fabricated by using the p(NIPAAm-*co*-PAA) polymers that were synthesized from the reaction of PAA and N-isopropylacrylamide (NIPAAM) via a reversible addition–fragmentation chain transfer.[69] Same as the aforementioned PBAE gel, the pH and temperature sensitivities were well exhibited by the p(NIPAAm-*co*-PAA) gel, but its swelling and drug liberation were promoted in high pH conditions. In pH 7.4 medium, this gel was dissolved within 4 days and completely released its loaded vascular endothelial growth factor (VEGF); when staying in acidic buffers (pH = 5 or = 6), the gel remained mostly undegraded even 28 days later and VEGF was liberated slowly and gradually. Moreover, a small decline of pH from 6 to 5 significantly accelerated VEGF release by p(NIPAAm-*co*-PAA) gel. Besides, the VEGF's cationic charge characteristic may affect its release from anionic injectable hydrogel under different pH values. At pH 6, VEGF was positively charged and strongly attracted by anionic groups of the p(NIPAAm-*co*-PAA) gel polymers, resulting in its tardy release; at pH 5, the carboxylic acid groups of polymers underwent protonation and became too few to keep VEGF, thus urging its discharge. Undoubtedly, such a VEGF-loaded p(NIPAAm-*co*-PAA) hydrogel would be especially able to act as a depot system at ischemic site to maintain a delayed but steady release of VEGF in that acidic tissue environment, thus gradually recovering hypoxic injury; and upon the return of tissue pH to normal value, the polymeric network of gel tends to dissolve away and disassembles finally.

Definitely, pH tunes the balance between attraction and repulsion inside the electrostatic interaction-supported hydrogels and alters their swelling. In an injectable hydrogel composed of silicate nanometer platelet, gelatin, and charged microgel,[60] laponite, a synthetic silicate nanoplatelet with plenty of surface negative charges and a small amount of edging positive charges strongly interacted with the gelatin chain with both positively and negatively charged regions and thus took gel shape. Premixing laponite with the positively charged chitosan or negatively charged PNIPAM-*co*-AA microgels before its gelling with gelatin could add additional electrostatic action to final gel network. Such a strategy nicely prevented the release of rhodamine under a pH range from 5 and 7.4 during a 475 h test, suggesting that any unwanted drug loss and toxicity may not happen in vivo. More notable is that this nanocomposite gel substantially degraded and liberated rhodamine drastically and rapidly at pH 9.18, a condition where gelatin and laponite became negatively charged and repelled each other.

Multivalent metal ions can form coordination bonds with nitrogen and oxygen atoms on polymer backbone and thus cross-link polymers in hydrogel. Coordination bonds break in a low pH environment, leading to the degradation of such type hydrogel.[44,76,77] Ni^{2+} were chosen to coordinate with the nitrogen atoms of four-arm poly(ethylene glycol)-*b*-polyhistidine (4PEG-PHis) to prepare a pH-sensitive injectable hydrogel in a neutral environment.[61] The protonation of the PHis chains under a pH below 6.0 could deprive their coordination with Ni^{2+} ions, disrupting the linkage between them and causing a gel-sol transition. Therefore, dissolve such gelation polymers in a medium with pH 5.8 for a syringe injection while deliver them into neutral environment (pH 7.4) to excite a sol–gel transition in situ. Of course, it would be reasonable to expect a fast drug release for this gel when endogenous pH drops to 5.5.

So far, all these types of pH-responsive injectable hydrogels have been intensively explored for real application in wounds, tumors, ischemia, and other lesions with enhanced lactate accumulation. The acid responsiveness is often combined with other gel sensitivity to achieve a better release control for therapeutic cargos at numerous pathological areas. Noticeably, ion interaction-supported pH-responsive gels may be interfered by clinical microinjection because they often lack mechanical stability and self-healing capability, which also limits their application to the elastic tissues that conduct constant expansion and contraction (e.g., lung, lung bed, and arteries) and to the interfaces with high stress.[12] In addition, the pH declines at therapeutic regions in cancers, wounds and infections are often not big enough to control drug liberation from many traditional acid-sensitive hydrogels,[78] so the pH responsiveness established upon dynamically chemical reaction appears to hold more potential in clinics.

3.1.2. Redox-Responsive Injectable Hydrogels

An increasing trend of ROS exists in various common pathologies, including inflammation, cardio- and cerebrovascular

© 2022 Wiley-VCH GmbH

diseases, neurodegenerative disorders, diabetes, and cancers.[79] To avoid oxidative stress, cells mobilize and promote their own reduction system, for example, producing antioxidative GSH, which elevates intracellular GSH to 2–10 mM, 1000 times higher than extracellular concentrations (2–20 μM).[80] No doubt, such redox dynamics in diseased tissues offer another kind of stimulation to injectable hydrogels.

Disulfide bond (–S–S–) is a strong covalent bond linking polypeptide chains in proteins. ROS oxidizes it into hydrophilic sulfoxide or sulfone while GSH reduces it to thiol, so most redox-responsiveness are designed as disulfide bond-dependent.[81] For example, Wang et al.[82] prepared a ROS-sensitive injectable hydrogel to release a therapeutical medicine tanshinone IIA (TIIA) as adapted to the inflammation-caused redox alternation in acute myocardial infarction (MI) (**Figure 3**). By using the "A2 + B4" Michael addition method, they first reacted diacrylate PEG 700 (DAPEG) with cystamine to synthesize the hyperbranched disulfide-containing poly(*β*-hydrazide ester (PBAE) macromers with multi-acrylate end groups. Afterward, they had dopamine polymerize around TIIA in a weak alkaline solution to generate TIIA@PDA nanospheres with a quinone-abundant surface. Mixing the prepared HB-PBAE macromers and TIIA@polymerized dopamine (PDA) nanospheres with the thiolate-modified hyaluronic acid (HA-SH) quickly formed the drug-laden hydrogel (HB-PBAE/HA-SH/TIIA@PDA) under a moderate condition via the sulfhydryl-addition reactions of thiolate with acrylate groups and quinone (Figure 3a). Such a dual chemical cross-link doubled and even tripled the modulus of hydrogels, warranting a fast gelation process and a high gelation fraction as displayed by good shape retention when gels were injected into PBS solution (Figure 3b). Numerous disulfide bonds of the HB-PBAE macromers endowed the final gel product a highly ROS-sensitive gel–sol transition since its degradation rate was much faster in 1 mM H_2O_2 than that in PBS (Figure 3c). To assess in vivo hydrogel degradation, the magnetic nanoparticles that were modified with PEI and then chemically linked onto the quinones of PDA were mixed into the hydrogel and sent into myocardium. As MRI imaging revealed, the hydrogel became slowly undetectable over time, with an 81% degradation rate during a 4 week period, suggesting a similar gradual TIIA release in myocardium. Excitingly, the injected HB-PBAE/HA-SH/TIIA@PDA hydrogels effectively increased the amplitude of left ventricular wall motion but inhibited ventricular dilation in myocardial infarcted rats. In fact, blank gel could already reduce the MI-enhanced myocardial fibrosis and collagen deposition significantly, indicating its ROS-scavenging activity; and further including TIIA better improved cardiac damage and reduced proinflammatory factor expression in a long term (Figure 3d).

On another side, disulfide linkages break under reductive pressure so the reducing agents such as GSH and dithiothreitol (DTT) also quicken the degradation of disulfide bond-based hydrogels and their drug release. This strategy was adopted for a reduction-responsive hydrogel to provide a transient support for defected bone regeneration and realize a desired induction of new bone formation by recombinant human bone morphogenetic protein-2 (rhBMP-2).[35] 4-arm-PEG molecules were modified into thiolated molecules and then oxidized in the presence of H_2O_2, rapidly gelling into disulfide bond-crosslinked hydrogels under moderate physiological conditions. As desired, the

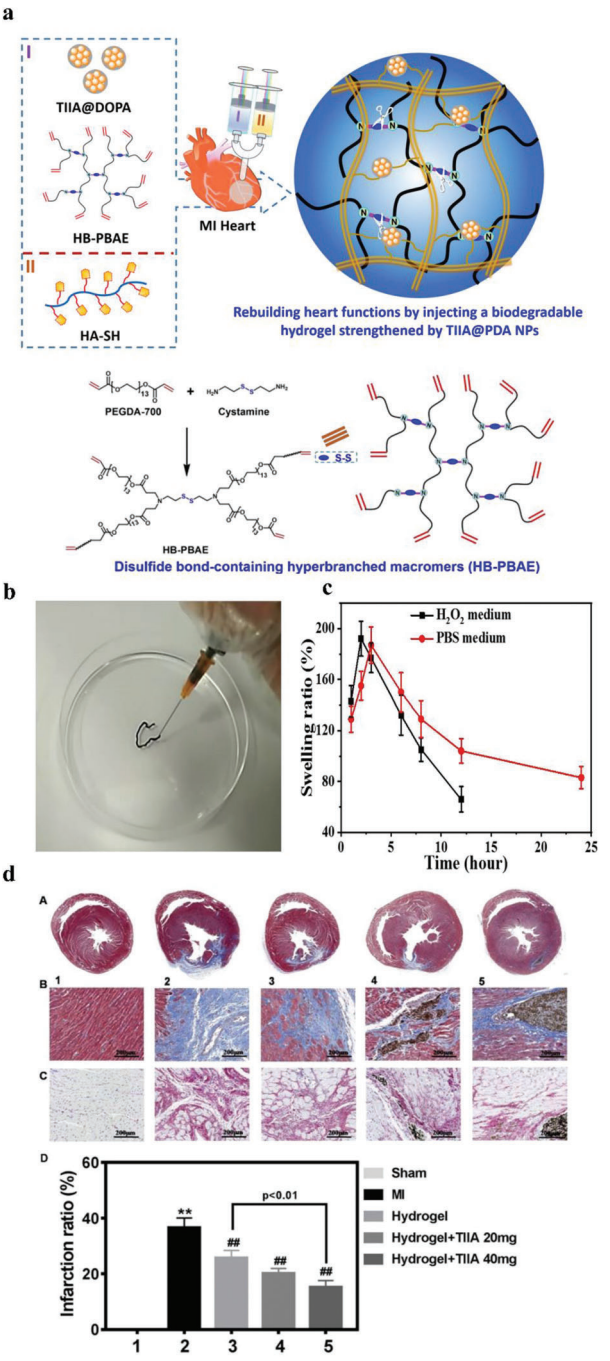

Figure 3. a) Top: Schematic illustration of the design of ROS-sensitive hydrogels cross-linked by TIIA@PDA nanoparticles to promote heart functions after MI. Bottom: Synthesis and characterizations of HB-PBAE. b) A typical picture of the injectable hydrogel. c) Swelling ratio of HB-PBAE/HA-SH hydrogels in PBS and 1 mmol L^{-1} H_2O_2 medium. d) Rebuilding postinfarcted cardiac functions by injecting TIIA@PDA nanoparticle-cross-linked ROS-sensitive hydrogels. Reproduced with permission.[82] Copyright 2019, American Chemical Society.

© 2022 Wiley-VCH GmbH

prepared hydrogel displayed a good injectability but also an elegant GSH-responsive disulfide breakage and gel disintegration. In contrast with a gradual increase in PBS, a "go up first and then down" profile appeared in the swelling ratios of the gel subjected to 0.01 mM GSH (a concentration mimicking extracellular GSH level), due to the earlier cleavage of disulfide bonds by absorbed GSH. Electron microscopy revealed that four-day immersion in 0.01 mM GSH significantly lowered pore interconnection inside gel body, and after 8 days' incubation, the hydrogel completely disintegrated, leaving micron-sized particles readily metabolized. Accordingly, the long-term release of the gel-carried BSA was significantly shortened in 0.01 mM GSH. Obviously, such a reductant-stimulated BSA release nicely suggests a controlled release of rhBMP-2 in vivo, which was indicated by better new bone growth in mice treated with rhBMP-2 loaded gels than that by cytokine alone. These rhBMP-2-carried hydrogels would be especially useful for tissue regeneration like bone since their responsive degradation not only creates a continual and gradual release of growth factors but also leaves room for the ingrowth like progenitors and hemocytes.

Of attraction is another novel redox-responsive drug carrier, the diselenide-based injectable hydrogel. Se (selenium), one element in the same main group of S (sulfur) in the periodic table, has a dynamic chemistry and redox responsiveness similar to sulfur. Better application in biological systems and material systems has been assumed for diselenide linkage-based hydrogels since diselenide bond energy is lower than disulfide bond and so its required dynamic chemistry condition seems to be milder than disulfide. A major obstacle to the development of diselenide-containing hydrogels is the poor solubility of Se-Se,[83] but Se-containing polymers are currently leaving their infancy and gaining good application in the fabrication of hydrogels[84,85] and micelles.[86,87] Nowadays, there have been several reported hydrogels with Se-Se-linkage that exhibit prominent ROS- and GSH responsiveness.[88,89] A representative is the injectable hydrogel formed by the mixing of 4-armed-PEG-succinimide glutaric acid esters and selenocystamines•2HCl.[88] This hydrogel degraded faster in the presence of H_2O_2 or GSH and the degradation rate went up along with the concentration increase of H_2O_2 or GSH. Nevertheless, there are only a few reports about double selenium bonds-based injectable hydrogels and further research and development are in need. Indeed, Mylotrag, a redox-responsive anti-CD33 antibody-linked drug developed by Celltech and approved for acute leukemia by FDA was withdrawn from the market since it failed to cure patients, highlighting the difficulty in redox-responsive drug control in complicated biological environment.

3.1.3. Enzyme-Responsive Injectable Hydrogels

The disease occurs with abnormal level of local enzymes that are highly specific and catalytically efficient for their substrates (peptides or nuclear acids) so can catalyze the degradation of the substrate-contained hydrogels. Based on different substrates, the enzyme sensitivity of injectable hydrogel are usually designed via peptide chain modification or DNA self-assembly.[90,91]

Types of MMPs are abundant in chronic inflammatory tissue and used as markers for the development of cardiovascular disease. Much effort has been made to develop the MMP-responsive hydrogel for treating MI, one clinically common critical illness. One hydrogel containing the MMP-cleavable peptide GGRMSMPV has been injected into Yorkshire pigs' hearts and achieved a controlled dose of recombinant tissue inhibitor of MMPs (rTIMP-3), nicely alleviating the induced myocardial infarction.[92] It was made from three macromers, the HA-aldehyde (HA-ALD), the dextran sulfate-aldehyde (DS-ALD), and the HA-peptide-HYD (HA-MMP-HYD), where the MMP cleavable peptides carrying sulfhydryl cysteine and hydrazine groups at both ends were conjugated to the HA-maleimide via thiol–maleimide click reaction. These macromers could rapidly cross-link together through Schiff-base reaction over a range of macromer weight percentages as 1–5% and yield the MMP-responsive hydrogels with a good viscoelasticity. As expected, though remaining pretty stable in PBS buffer, the prepared gels (3.5 wt%) kept only one-fifth of their original weight in the presence of 20 U mL^{-1} type 4 collagenase on the 12th day. Correspondingly, collagenase speeded up the release of the gel-carried BSA almost twice as fast as that in PBS, leading to BSA liberation close to 100% in the end of incubation. Moreover, it took only 2 days to realize a full gel degradation and BSA emancipation when collagenase concentration elevated tenfolds, further verifying a wonderful MMP responsiveness of such gels. Excitingly, these rTIMP3-laden gels maintained this susceptivity after being injected into pig's heart since no trace amount of hydrogel in the MI pigs was revealed by magnetic resonance imaging (MRI) and histological examination 14 days' post injection, while substantial gel products were left in the camouflaged animal's tissues. More encouragingly, the MI pigs introduced with rTIMP3-laden gel displayed a wide improvement in left ventricular ejection fraction, chamber dilation, MI thickness, and progressive increase in pulmonary capillary wedge pressure, strongly demonstrating the potential of MMP-responsive injectable hydrogel in treating heart attack.

Free fatty acids have recently been utilized for responsive hydrogel since their ester linkages become labile and dissociated under high levels of MMPs in certain pathological conditions. Triglycerol monostearate (TG-18), a FDA-approved medical agent with a hydrophilic polyhydroxyl head group and a hydrophobic polymethylene tail, was employed to yield an arthritis flare-responsive hydrogel in order to titrate a drug release to match the periodic disease activity of inflammatory arthritis.[93] Amphiphilic TG-18 assembled into micelles via hydrophobic interaction and was dissolved in hot dimethyl sulfoxide/water, and the following cooling extended TG-18 lamellar structure into higher order fibrous assemblies to form solid hydrogel. Such TG-18 hydrogel was evidently injectable and highly biosafe for chondrocytes or synoviocytes from healthy and rheumatoid arthritis (RA) human joints, but its MMP responsiveness was the most impressive. In the presence of MMP-2, -3, or -9 with the concentrations corresponding to their levels in RA patients' synovial fluid, the release of gel-entrapped corticosteroid triamcinolone acetonide (TA) or 1,1′-dioctadecyl-3,3,3′,3′-tetramethylindotricarbocyanine iodide (DiR) fluorescent dye was significantly faster, while the addition of MMP inhibitors completely eliminated this promotion. Exposing TG-18 gel to synovial fluid from RA patients' joints perfectly reproduced this response, suggesting that it could conduct degradation and drug release as needed to adapt inflammatory

© 2022 Wiley-VCH GmbH

status in vivo. In agreement, the intra-articularly injected TG-18/DiR gels disassembled much faster in arthritic K/BxN mice than healthy animals, and the decay of DiR signals turned quicker when more severer arthritis induced, showing that TG-18 hydrogel is responsive to arthritis flare activity in vivo and carry out on-demand disassembly and drug release. Such perfect responsiveness aided it to achieve an outstanding anti-inflammatory effect and a large reduction of K/BxN serum-induced arthritis in mice. More pleasingly, it was found that just a single injection of TG-18/TA at the peak of disease severity could produce enough efficacies even for severe arthritis, highly marking the promise of TG-18 hydrogel as well as other fatty acids-based gel as a drug delivery system in treating IA and other diseases.

Additionally, endogenous nucleases have been employed to control the degradation of nuclear acid-linked hydrogels and their drug release. Double-stranded helical DNA molecules are widely used to construct injectable hydrogel because of their strict base complementarity, sequence-dependent programmable assembly, good biocompatibility, adjustable responsiveness, and perfect chemical modification.[94,95] In the body, DNA hydrogels are degraded by nucleases and gradually decompose into nano-sized particles, thereby nicely penetrating into pathological tissues and into diseased cells deep in tissue. Such an advantage of DNA gels is extremely applicable for solid tumors with a relative large size or thick ECM protection since the reach of common drugs for tumor interior becomes poor due to defective intratumoral vascular network and ECM blockade. Zhang et al.[96] took use of the DNAs coupled with camptothecin (CPT) to fabricate a CPT-laden injectable hydrogel and produced a successful antitumor effect in the xenografted animals (**Figure 4**). They divided six oligonucleotides (oligos) into two groups and elaborately designed each oligo to encompass three segments: Two consisting of sequences respectively complementary to two other oligos and one with "sticky end." Three oligos in each group could according to their own complementarity assemble into a Y-motif (Y1 and Y2, respectively) with the same sticky end in three different directions, and the sticky ends of two motifs could exactly complement each other. Phosphorothioates were further introduced into the nucleotides of single stranded DNA molecule (ssDNA) and mediated the conjugation of disulfide-modified camptothecin onto the ssDNA backbone. After heat denatured, these CPT-ssDNAs would yield two groups of Y-shaped building blocks that link with each other via their complementarity sticky ends and thereby rapidly generate the CPT-laden DNA hydrogels (Figure 4a). Unsurprisingly, these CPT-DNA gels were readily squeezed out of the 26-gauge needle (Figure 4b), exhibiting a good injectability. As hoped, 12 h digestion of DNA gels with DNase I released small particles into the supernatant while no significant degradation took place in the absence of DNase I; and the particle size was reduced from 1 μm to ≈130 nm along with increasing enzyme concentration from 5 to 30 U mL^{-1} (Figure 4c). Consistent with their good enzymatic- and GSH-responsiveness shown in vitro, the intratumorally injected CPT-DNA-gels generated excellent long-term cytotoxicity to tumor cells deeply sited in tumor blocks and effectively inhibited the recurrence of 4T3 xenografts in male nude BALB/c mice (Figure 4d). Obviously, the DNA materials own many excellent properties to support their application in injectable hydrogels for drug delivery and release. In fact, more and more attention has already paid to such gels and their preparation has been intensively reviewed somewhere else.[97]

3.1.4. Glucose-Responsive Injectable Hydrogels

The prevalence of diabetes mellitus makes its treatment become urgent. Insulin is commonly used and effective for type I diabetes but its repetitive intravenous injection greatly reduces patient compliance. Hydrogel encapsulation enables a prolonged and sustained insulin release.[98] During passing decades, glucose-responsive injectable hydrogels have been developed to act like closed-loop insulin delivery systems, monitoring blood glucose fluctuation and releasing as on-demand insulin in a real time way. Currently, glucose responsiveness to injectable hydrogels is either basing on electrostatic repulsion due to the protonation of polycationic gelation molecules when glucoses are oxidized to gluconic acids by glucose oxidase, or depending on the competitive binding of glucose through their diol functionality to boronate anions and the resultant disassembly of covalent boronate ester-crosslinked hydrogels.[37]

Diabetic foot ulcer features with a prolonged inflammatory phase that causes a low pH and high glucose microenvironment and further delays wound healing. To copy with such pathological situations, phenylboronic acid (PBA)-modified chitosan, poly(vinyl alcohol), and benzaldehyde-capped PEG were used as raw materials to produce a glucose- and pH sensitive injectable hydrogel where phenylboronate ester bonds and Schiff base linkages cross-linked three classes of macromolecules together.[99] As expected, decreasing pH from 7.4 to 6.8 or increasing glucose concentration to 50 mM reduced the modulus of this hydrogel significantly. In immersion experiments, the accumulative release of insulin at a release time of 34 h rose from 9% at pH 7.4 to 33% and 43% at pH 6.5 and pH 7.4 containing 3 mg mL^{-1} of glucose, respectively, suggesting that the diffusion of insulin does not simply follow Fick's law any more under an acidic and hyperglycemic condition. Consistent with such a responsive release of insulin, the best healing effects were obtained by insulin and the fibroblasts when both were applied via the responsive injectable hydrogels to the wounds on the back of STZ-induced diabetic rats. During the 18 days post-wounding, the animals treated with insulin/L929-loaded hydrogel were seen to carry the lowest blood glucose level and largest shrinkage of wound area, which was obviously due to the dual responsive release of insulin and fibroblast that best induced inflammatory cell infiltration, neovascularization, cell proliferation, and collagen deposition in wounds. Assuredly, as one of the most promising insulin delivery systems, the PBA-based hydrogels hold the potential to really replace cumbersome insulin injection in future as long as effective improvements are achieved for their responding rate, tissue adhesion, and unwanted leakage under normoglycemic conditions.[100,101]

As discussed earlier, the glucose oxidase-catalyzed conversion of glucose into gluconic acid would acidify microenvironment and trigger the protonation of groups similar to amino groups. A glucose-sensitivity was introduced into the pH-sensitive self-assembling peptide hydrogel (renamed as peptide IA-0) by this approach.[102] IA-0 peptide was rigidized by the replacement of its valines with more hydrophobic isoleucines and became more

© 2022 Wiley-VCH GmbH

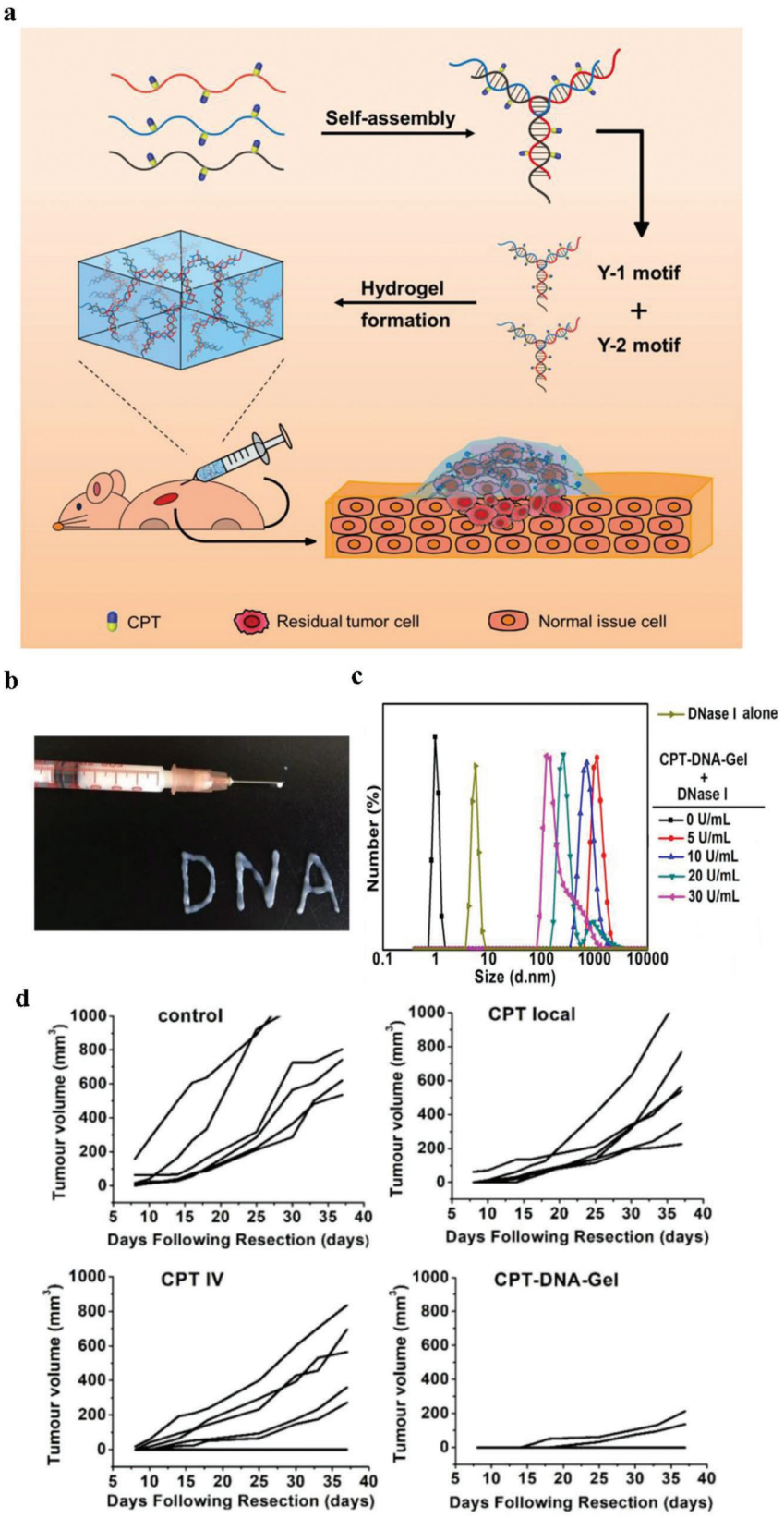

Figure 4. a) Schematic illustration of the synthetic route of CPT-conjugated DNA hydrogel. b) The injectable property of CPT-DNA-Gel. c) Nuclease-induced digestion and disassembly of CPT-DNA-gel in the presence of DNase I. d) Growth of the recurrence tumors after tumor resection. Reproduced with permission.[96] Copyright 2020, American Chemical Society.

© 2022 Wiley-VCH GmbH

propense to perform β-sheet hydrogen bonding, thus prompting its self-assembly under physiological condition to form injectable hydrogel laden with insulin, glucose oxidase, and catalase. Upon the entry of glucose into gel, gluconic acid was produced and accumulated in gel body, protonating adjacent alkaline amino acids of side chains, leading to their repulsion from each other, and eventually causing gel collapse and the subsequent release of insulin. Indeed, solution pH value gradually dropped along with the rise of glucose concentration from 0 to 400 mg dl^{-1} during 12 h immersion and was lowered to about 5.9 only 6 h later if gel was left in 400 mg dl^{-1} glucose solution, indicating the proton accumulation and the generation of an acidic environment that sufficiently triggered hydrogel disassembly. In agreement, it took only 12 h for protein gels to emancipate almost half of the carried fluorescein isothiocyanate isomer (FITC)-insulin in 400 mg dl^{-1} glucose solution, whereas very few FITC signals were detected in PBS or 100 mg dl^{-1} glucose solution. Attractively, the therapeutic performance of the subcutaneously injected enzymes-carried hydrogels (G(E+I)) in the STZ-induced diabetic mice beat anyone with insulin alone (G(I)) in many ways. For example, the blood glucose of G(E+I)-treated mice was maintained within normal range (11 mM, non-fasted conditions) for 4 days and these hypoglycemic effects lasted for a maximum of 6 days; oppositely, the mice with enzyme-minus gel had significantly higher blood glucose levels.

3.2. Injectable Hydrogel Reactive to External Physical Stimuli

Besides endogenous signals, the responsiveness to physical stimuli such as light, magnetic, electrical, and ultrasound have been brought into injectable hydrogels for drug delivery and controlled release.[18] Obviously, an accurate manipulation of response degree becomes accessible to generate on-demand drug doses and thus maximizes therapeutic efficacy by adjusting relevant parameters (e.g., frequency, intensity, duration, power, etc.), and photo-, magnetic-, and ultrasound stimulation all generate heat to intervene physical interplays of gelation molecules such as host–guest and electrostatic interactions, and then control drug release, so thermal efficiency becomes the research focus of such responsive hydrogels.

3.2.1. Light-Responsive Injectable Hydrogel

Light is easily acquired, operated remotely, and strongly manageable, so light radiation became one of the most popular medical intervention approaches.[109] In fact, applying photostimulation to control gel formation and biodegradation has been undergoing for quite a while.[103] Light sensitivity of injectable hydrogel is extremely attractive since the precisely controlled drug release could be easily realized in an endogenous environment via elaborately designing power density, wavelength, beam diameter, and exposure time.[104] Generally, gel structure and drug release alter due to light-transformed heat or to the photolabile backbones.

Photothermal Injectable Hydrogel: Many photothermal agents with small phototoxicity and good penetration, like rare metal nanostructures,[34,105] organic nanoparticles,[106] and black phosphorus nanoflakes,[107] have been introduced into and provided injectable hydrogel with safe photothermal activity for an apt control of drug release. A major concern for this type of hydrogels is the thermal damage to cells since intense heat (above 50 °C) causes cell necrosis while heat shock proteins may heal the injury from low heat (from 44 to 47 °C). Therefore, the intensity and duration of light irradiation should be carefully explored for photothermal hydrogels, different therapeutical targets, and surrounding normal cells and tissues.[108,109]

Platinum (Pt) nanoparticles own a good photothermal conversion efficiency and biocompatibility so are popularly applied into photodegradable hydrogels. To fabricate a NIR light-responsive, degradable, injectable hydrogel for controlled drug delivery, Wang et al.[34] first conjugated a high density of PEG chains on the surface of poly(amino amine) dendrimers that were later used as a template to synthesize ultrasmall Pt nanoparticles. When mixing with α-cyclodextrin (α-CD), such prepared DEPt-PEG materials generated multiple pseudo polyrotaxane (PPR) beads via the host–guest inclusions between α-cyclodextrin (α-CD) and PEG and further formed supramolecular hydrogels through hydrogen bond interactions between these PPR assemblies. Since the de- and re-threading of α-CD from PEG were heat sensitive, the DEPt-PEG/α-CD hydrogels well featured with thermosensitive degradation and reversible cross-linking, supporting their injectability and laser irradiation-controlled gel degradation and drug release. As expected, a NIR irradiation with a power density of 0.62 W cm^{-2} could heat such hydrogels from 26 to 46 °C within 20 min but not warm the ones without Pt nanoparticles at all. Accordingly, though the Pt-lacking ones remained solid during the whole exposure, the Pt-containing gels completely degraded by irradiation and nicely consisted with the irradiation-triggered release of anticancer drug bortezomib (BTZ) in vitro as well as of cyanine 5.5 in tumor-xenografted mice. Evidently, the included Pt nanoparticles could effectively drive the hydrogel-based drug delivery system to spit out the entrapped therapeutic agents in an on-demand and dose-tunable fashion in the body.

However, the conversion efficiency of metal nanoparticles declines after being embedded into the gel so the laser to excite them often have to be high or even beyond skin tolerance threshold. To elevate photothermal efficacy and avoid laser injury, researchers have tried to conjugate photosensitive agents to the backbone of gelation polymers and obtained a more direct photothermal conversion in the gel and a gel–sol transformation with NIR irradiation. For example, the poly(*N*-phenylglycine) (denoted as PPG) was first synthesized from the photoreactive *N*-phenylglycine under chemical oxidation and then modified with methoxy-PEG-amine via amidation condensation.[110] The PEGylated PPG polymers (PPG-peg) not only provided photothermal polymeric backbones, but also formed the thermosensitive PPR assemblies via the famous host–guest inclusion between PEG and α-CD and the photothermal-network hydrogels (PNT gel) via PPR interaction (**Figure 5**a). Similar to other hydrogels maintained by electrostatic interaction and coordination bonds, such fabricated PNT-gel underwent matrix disruption when subjected to the syringe's shear force, turning into injectable fluid material with a low viscosity (Figure 5b). Moreover, they had a strong adsorption in the NIR region that peaked at 630 nm, obviously due to the charge transfer in the benzene rings of phenylglycine. Correspondingly, 5 min exposure to an 808 nm laser with a low power density of 0.3 W cm^{-2} quickly heated the PPG-peg solution and

© 2022 Wiley-VCH GmbH

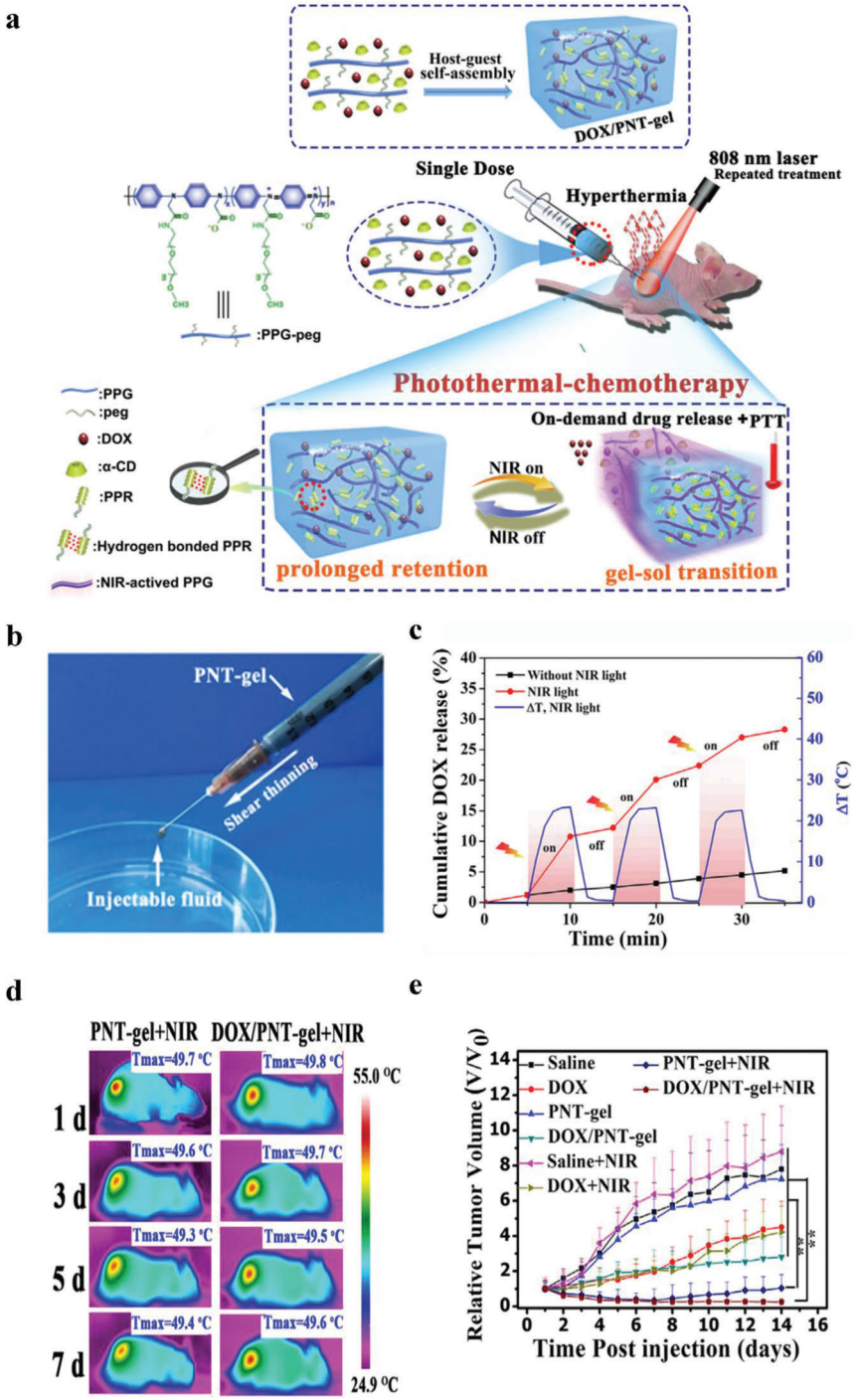

Figure 5. a) Schematic illustration of the fabrication of the supramolecular PNT-gel and its application for repeated photothermal-chemotherapy via one-dose injection followed by multiple treatments. b) Digital photograph showing the shear-thinning and injectability of PNT-gel. c) Release of DOX from the hydrogel with pulsed laser irradiation (808 nm, 0.3 W cm^{-2}) and the corresponding photo-triggered temperature elevation.d) Infrared thermal images of mice taken at the maximum steady temperatures during treatment (808 nm; irradiation time: 5 min; power: 0.15 W cm^{-2}). e) Tumor volume changes over treatment. Reproduced with permission.[110] Copyright 2019, Elsevier.

© 2022 Wiley-VCH GmbH

the PNT-gel to 46.5 and 50.8 °C, respectively. Along with irradiation lasting for 25 min was the gradual transformation of the PNT gel into a flowable solution phase and the loss of gel mass down to 8.2%, markedly demonstrating that NIR laser heated and disrupted host–guest assembly to trigger gel–sol transition. Consistent with this, the release rate of gel-encapsulated DOX significantly differed before and after laser irradiation, with a 28% release after four on/off irradiation cycles, contrasting to a 5% yield without laser irradiation (Figure 5c). Cytotoxicity assay in L929 cells and 4T1 cells also revealed that the drug-loaded hydrogels turned lethal shortly after irradiation and decreased cell viability with increasing irradiation time. Encouragingly, though the signal of the laden fluorescent molecule decayed very slowly and remained distinct even 14 days after injection without irradiation in the xenografted tumors, 5 min long NIR radiation rapidly increased the temperature of tumor sites introduced with the PNT gels close to 50 °C the next day of injection, and such a warming effect remained almost unchanged during the following 6 days (Figure 5d). Consistently, tumor volume was reduced markedly by NIR irradiation in all mice carrying the PNT gels. More pleasingly, tumors appeared to stop grow during the two-week test in the PNT-gel + NIR group and even declined when DOX was further included, indicating that combining chemotherapy with PTT (photothermal therapy) can yield much better anticancer effects (Figure 5e). Notedly, the DOX carried by PNT-gel produced a stronger suppression of tumor when compared to the naked drugs, suggesting that its release was indeed under the control of the PNT gel in vivo.

Injectable Hydrogel with Photo-Unstable Skeleton: Light can directly act on the light-unstable polymers of injectable hydrogels to accelerate their degradation.[111,112] For example, UV caused the disintegration of photolabile gelation polymers where the 4-arm PEG were modified with UV-destroyed 2-nitrobenzyl (NB) ester bonds.[113] Such macromolecules solidified into a gel within tens of seconds under the catalyzation of horseradish peroxidase and H_2O_2 and degraded under UV irradiation at 10, 50, and 100 mW cm^{-2} within 6, 4, and 3 h, respectively. However, the amount of H_2O_2 used for gel injection was too much to be safe for cells in this report.

UV-lability is inapplicable for injectable hydrogel to go deep tissues accessible only by long wavelength light, which then prompted the development of NIR-responsive molecules and hydrogels. A ROS-degradable HA-based hydrogel exhibited how NIR irradiation affected gel structure and degradation and adjusted drug release by exciting singlet oxygen.[114] This HPTG hydrogel was formed via the reversible Schiff base reaction between adipic dihydrazide hyaluronic acid (ADH-HA) and dialdehyde-functionalized ROS-cleavable thioketal linker (TK-CHO), and the partial hydrazide groups of ADH-HA were covalently conjugated through amidation reaction with a water-insoluble photosensitizer popularly applied in clinics, protoporphyrin IX (PpIX), to achieve a good dispersion for PpIX and an effective PDT. Under NIR radiation, PpIX excited extensive singlet oxygen production, which not only carried out PDT for cancer cells but also cleaved the thioketal linkers of TK-CHO to disrupt the cross-linking of HAs in gel body. As expected, the conjugation of PpIX to polymers effectively elevated their irradiation-induced singlet oxygen production when compared to free PpIX in aqueous solution, while the disruption of the disulfide bonds of TK-CHO occurred simultaneously, turning 18% and 46% of the TK-CHO to acetone, 4-hydroxybenzaldehyde or oxidized derivatives in 5 and 10 min, respectively. Correlating with such a NIR irradiation-sensitivity of the HPTG was their NIR light-tunable degradability and cargo release kinetics. After NIR irradiation, these gels were found to not only decompose much greater in vitro but also release the encapsulated DOX or gold nanorods more rapidly, whereas their two light-insensitive counterparts, the HPAG lacking the thioketal linker and the PpIX-unconjugated HATG, appeared to be affected a little. Furthermore, intratumorally injected HPTG gels yielded intense signals of encapsulated fluorescence probes in 4T1 tumor-bearing mice and remained their detectability over 15 days at injection site, whereas there was only weak fluorescence intensity produced by free PpIX, seemingly due to the obvious aggregation and severe self-quenching of free PpIX. Correspondingly, NIR irradiation triggered antitumor effects in all mice treated with PpIX, including free PpIX, the HPTG, and the DOX-loaded HPTG, and the irradiated tumors treated with DOX-loaded HPTG gels almost stopped their growth during 18 days. Certainly, such an impressing combined chemo-photodynamic cancer therapeutical strategy indicates the brilliant future of the light-controlled hydrogel-based drug delivery.

3.2.2. Magnetic Responsive Injectable Hydrogels

Recently, there has been a rapid development of composite hydrogels consisting of superparamagnetic nanoparticles or particles (e.g., Fe_3O_4, γ- Fe_2O_3, $CoFe_2O_4$). Since such particles would do directional movement and get close to each other in the external magnetic field, the drugs embedded into gel inside could be easily squeezed out.[115,116] The heat from the magnetic relaxations of these paramagnetic particles under an alternating magnetic field could also warm up gels and drive the release of cargos.[117]

$Fe(Oleate)_3$ was encapsulated into pluronic F127 micelles to fabricate superparamagnetic iron oxide nanoparticles (SPIONs).[118] Pluronic F127 copolymers consist of one poly(propylene oxide) (PPO) block and two poly(ethylene oxide) (PEO) blocks, staying as a "'sol"' at 20 °C but transforming into gel due to stronger hydrophobic interaction at high temperatures like 36 °C. SPION hydrogel reduced its length from 2.39 to 2.22 cm after being exposed to the MF (300 mT) for 2.5 h, indicating that the hydrophobic cores inside of the gel were "squeezed" significantly in a magnetic field by the orientational attraction of SPIONs. The local concentration of the indomethacin in the PPO hydrophobic cores of pluronic F127 micelles was gradually rising during the exposure to the external magnetic field.

In another magnetic supramolecular hydrogel (MSH), anticancer drug paclitaxel (PTX) and DOX were carried and manipulated to release via magnetothermal effects.[119] In this system, the PEGylated Fe_3O_4 nanoparticles were readily included into α-CD and generated the injectable MSH gel where PTX tightly bound to the hydrophobic part of the PEGylated Fe_3O_4 nanoparticles while DOX was wrapped in the hydrophilic compartment. As hoped, 5 min irradiation with an alternating current magnetic field (ACMF) could significantly raise the release of two drugs from the MSH, elevating the cumulative release from 3% to 13% for PTX and from 49% to 63% for DOX on the first day. Evidently, such a responsiveness of the MSH was established upon

© 2022 Wiley-VCH GmbH

the magneto-thermal activity of the PEGylated Fe_3O_4 nanoparticles that warmed the MSH up to 45 °C, a critical temperature that would rock the inclusion complexation structures of the MSH and finally resulted in gel–sol reversible transition and the discharge of chemotherapeutic drugs. The MSH could also conduct a pronounced thermal killing similar to conventional tumor magnetothermal therapy and light-responsive injectable hydrogels in cancer cells, suggesting that it would synergize with chemotherapeutic drugs to further amplify cytotoxic effects. Additionally, supramolecular MSH gel possessed a thixotropic property that underpinned its shear thinning behavior, injectability, and self-healing capability.[120]

Distinguishing the magneto-reactive injectable hydrogels from other types of response systems is that magnetic nanoparticles or particles can serve as MRI contrast agents,[121] which can be used to evaluate gel degradation and monitor the surrounding tissue conditions through multi-parameter MRI, thus enabling a real-time observation of disease development.

3.2.3. Electrical Responsiveness Injectable Hydrogels

Electrical activity is one ordinary phenomenon to preserve cell homeostasis and intracellular development.[122,123] Due to its great operability, electrical stimulation may be the most manageable approach for gel carriers to highly and accurately control the drug release and so becomes a very attractive reactivity for hydrogel-based delivery system. Studies have shown that conducting hydrogels could modify the impulse propagation at the site of myocardial infarction and restore the synchronous contraction of myocardium.[124] Moreover, conductive polymers become charged under electrical field and thus freely interact with nerve cells, affecting cell adhesion, and neurite lengths.[125] So, electrical responsiveness is especially suitable for drug delivery systems applied to biomedical treatment of MI and nerve damage.

The electrical responsiveness of hydrogel is established upon a variety of gelation polymers with good electrical activity and processability, such as conductive polymers like polypyrrole and polyaniline.[126] Their electronic conductivity is usually dependent on their conjugated π systems (i.e., π–π stacking) and the overlap of π orbitals by the polymerization of polymer chains. The stacking of aromatic rings creates many conjugated π systems for polymers, prompting delocalized electrons to transfer along chains or between conducting polymer chains of hydrogel. The higher the transfer capability of charge along polymer chains, the stronger the electrical conductivity endowed to gel.[127–130] Under electrical stimulation, the drug release from such conductive hydrogels mainly follows two mechanisms: i) directional movement to opposite charge; ii) being expelled by the shrinking hydrogel.[131]

The first strategy was used to prepare electrical-responsive injectable hydrogels by conjugating the chitosan-grafted polyaniline (CP) with the oxidized dextran (OD) via the Schiff-base reaction. Polyaniline is a well-known organic semiconductor, exhibiting both electronic and ionic conductivity.[132] The CP polymers were seen to carry out a continual transition between oxidative and reductive states and lead to reversible ion exchange, transforming whole gel body into a conductor. During this electrochemical reduction, charged drug molecules migrated in an electric field, left the CP/OD hydrogel and further moved toward the electrode with opposite charge, resulting in the complete drug escape from the hydrogels. Unsurprisingly, applying 1 and 3 V voltages to the CP/OD hydrogel for 80 min raised the release rate of the loaded amoxicillin and ibuprofen from 34% (without voltage action) to 69% and 82%, respectively; furthermore, the CP/OD gels liberated about 18%, 14%, and 5% amoxicillin under three electrical stimulations and 5%, 4%, and 2% ibuprofen as well, suggesting that "on–off" pulse stimulation with multiple intervals (on for 3 min vs off for 60 min). The CP/OD hydrogels realized a precise release control of their cargos simply by adjusting the applied voltage parameters.

It is worth to mention that electrical stimulation therapy has been applied in clinic. Low frequency pulse current with certain intensity can induce muscle movement to relieve muscle spasm, prevent muscle atrophy, increase blood circulation, and maintain or enhance motion range. It also helps patients who suffer stroke or spinal cord injury to restore the ability to stand, walk, stretch, and grasp.[133] Therefore, dual therapeutic effects may be expected for the conductive hydrogel-based drug delivery system.

3.2.4. Ultrasonic-Response of Injectable Hydrogels

As one sound wave with a frequency higher than 20 000 Hz, an ultrasound wave is characterized with good directionality, strong reflection ability, easy access to more concentrated acoustic energy, and long propagation distance in the water. In particular, ultrasound can effectively penetrate tissues with a relatively high spatial and temporal resolution, so has been considered to act as a convenient stimulus.[134] Actually, ultrasound has been used to disrupt the physical cross-linkings that maintain the hydrogel framework[135] and the structure of the nanoparticles embedded into the injectable hydrogel.[136] Besides, ultrasonic mechanical vibration would excite high-frequency friction on the surface of objects, generating heat to enhance gel swelling and degradation as well as drug liberation.[137]

A clever application of ultrasound to control the drug release from hydrogel was given by Huebsch et al.,[138] who created hydrogels with alginic acid and divalent cations (Ca^{2+}). In this gel system, the ionic linkage of divalent calcium ions with alginate got lost under the action of ultrasound wave but could be restored by abundant Ca^{2+} in body fluid upon the removal of ultrasonic stimulation, therefore producing an ability for such gels to conduct a reversible on-demand drug release (**Figure 6**a). Indeed, ultrasound administration (9.6 mW cm^{-2}, 5 min pulse, once per hour) greatly promoted the liberation of the loaded mitoxantrone from these alginate hydrogels, escalating both release rates and accumulative release with an ultrasonic periodicity (Figure 6b). To assess the therapeutic efficacy of such a gel-drug system, the tumor-bearing nude mice were subcutaneously injected with gels and cargos and given a 2.5 min ultrasound treatment on the next day via an ultrasound transducer attached to the underlying alginate hydrogel and a Sonics Vibra-Cell VCX130 sonicator (13 mm diameter horn, 120 mW cm^{-2}). As expected, the area blued by the mitoxantrone that was released and deposited in peritoneal cavity was larger in the ultrasound-treated group

© 2022 Wiley-VCH GmbH

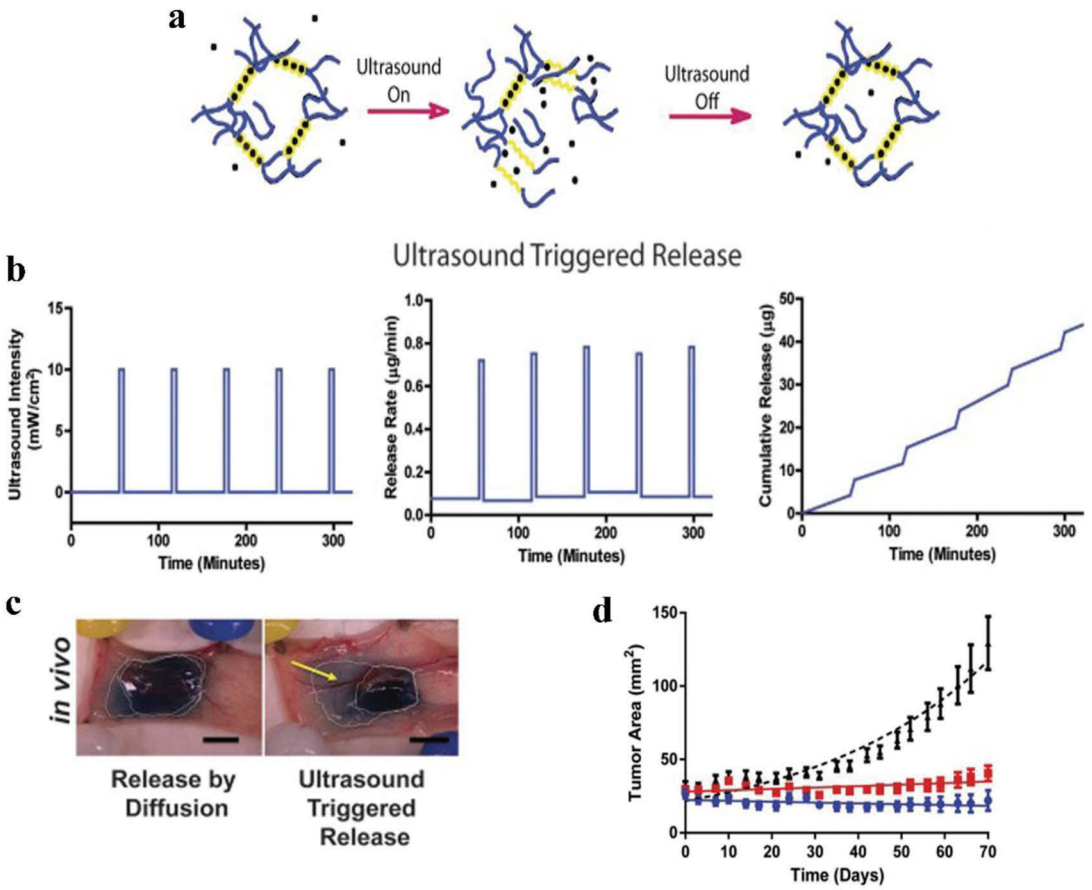

Figure 6. a) Schematic of the proposed ability of ultrasound to induce transient disruption of hydrogels cross-linked by calcium, followed by the reformation of cross-links by calcium within physiologic fluids, resulting in gel healing. Calcium (•) binds selectively to guluronic acid chains (yellow) of alginate polymers. b) Quantitative analysis of mitoxantrone release via ultrasound treatment (5 min, applied once every hour). Data indicate ultrasound intensity (left), mitoxantrone release rate (center), and cumulative mitoxantrone release (right). c) Representative images of residual mitoxantrone contained in alginate hydrogels, and mitoxantrone released from gels and subsequently deposited into host tissues, after hydrogels were transplanted into Nu/J mice and treated once with ultrasound for 2.5 min (right) or left untreated (left) over a 24-h period. d) Growth curves for human MDA-MB-231 breast cancer xenografts in Nu/J mice. Tumors were left untreated (black curve), exposed to a standard alginate gel loaded with mitoxantrone but not ultrasound (red curve), or treated with a combination of mitoxantrone-laden hydrogels and daily ultrasound (blue curve). Reproduced with permission.[138] Copyright 2014, United States National Academy of Sciences.

compared to the untreated ones whereas the size of remnant gel was much smaller, indicating that ultrasound significantly accelerated gel degradation and prompted drug feeding (Figure 6c). In correspondence, these drug-laden hydrogels produced a cytotoxic response positively correlating with ultrasound level in MDA-MB-231 cells; and after transplanted into the tumors xenografted by MDA-MB-231 cells, they more effectively inhibited tumor growth in combination with daily ultrasound therapy as observed on day 7, and this enhancement in antitumor effects became more and more obvious during the following 8 weeks (Figure 6d).

Instead to break the gel matrix structure, ultrasound also ruins the nanoparticles encapsulated into the injectable hydrogel and promote drug leaving.[136] Such an injectable gel was formed via the Schiff' base reaction between carboxymethyl chitosan and oxidized chondroitin sulfate, while the poly (lactide-*co*-glycolic acid) microspheres carrying chondrogenesis-inductive drug kartogenin (MPs@KGN) were embedded into gel matrix via ultrasonication. As designed, the MPs@KGN assembly would undergo disaggregation under ultrasound action, leading to a quick release of KGN. When these gel scaffolds were incubated with rat bone marrow mesenchymal stem cells (rBMSMCs), the most obvious chondrocytic phenotype appeared in the CMC-OCS@MPs@KGN/Ultrasound group since these cells produced the strongest staining for collagen II, indicating that ultrasound triggered more KGN from gel scaffold to differentiate MSCs into chondrocytes.

Ultrasound is used extensively for medical diagnosis and treatment such as surgery, obstetrics and gynecology, weight loss, stones, and birth control, so introducing ultrasound-responsiveness into gel carriers may enable not only the controlled release of drug but also real time monitoring of therapeutic effects at lesion tissues.

Overall, the frequency, strength, and irradiation area of the aforementioned external stimuli would be explored and optimized to avoid the damage to normal tissues and to prevent gel collapse and drug burst. In particular, the best magnetic and irradiative technologies are needed to be decided to reach a sufficient intensity at the lesion area.[139]

© 2022 Wiley-VCH GmbH

4. Conclusions and Future

In summary, the stimuli-responsiveness would greatly improve the controlled release of drugs from hydrogel reservoir and produce the best doses to suit various therapeutic needs and minimize side-by effects. Each responsiveness strategy has its own advantages to favor their specific application, but the perfection of the responsiveness of gel system is going on all the time. Combining the sensitivities to two or more stimuli obviously holds a big future for gel carriers since it may allow more precise control of gel degradation and drug escape. Especially, applying chemical or biochemical and physical stimulation simultaneously has been shown to enable an on-demand drug release and integration of diagnosis and treatment.[83,140] The curative success of responsive injectable hydrogels in animal disease models also supply promise for their future use in clinics.[14] However, the execution and performance of these responsiveness largely rely upon our perception of the disease circumstance which not only derives stimuli but also mediates and determines the action of external stimulation. In particular, the endogenous stimuli, such as pH value of tumor tissues and antioxidants in blood, vary in persons and are hard to control. Therefore, deepening our knowledge of disease pathology is always critical for the design and development of the reactivity for gel delivery system.

Compared to endogenous stimuli, external stimulation including light, magnetism, electricity, and ultrasound, is far more manipulable and able to realize an on/off pulsed drug release behavior for injectable hydrogels. The sensitivity to the light capable of penetrating deep tissues would be the future development direction for photo-responsive hydrogel, while the magnetic gel can serve as drug carrier and visualization mediator to achieve a real time monitor for treatment. Interestingly, light, magnetism, and ultrasound are all thermogenically active, which favor gel degradation and drug release but may also make health cell and tissues under the risk of thermal killing. Therefore, great attention and effort should be given to the control of heat production when applying the injectable delivery gel products with these responsive features to lesions. In addition, how healthy cells and tissues respond to this external stimulation deserves intensive investigation since most living components of the body answer these signals to different extents.

It is worth to mention that there are more endogenous signals appearing able to act as promising candidate stimuli for the hydrogel responsiveness, such as nitric oxide (NO) and nitrite. NO alters its level during vasodilation, neurotransmission, and inflammation. The first NO-responsive hydrogel was already obtained via a NO-cleavable cross-linking agent (N,N-(2-amino-1,4-phenylene) diacrylamide.[141] On the other side, the 4-substituted dihydropyridine derivatives with nitroso ions were employed to make a NO_2-sensitive hydrogel.[142] Overall, along with our comprehension of disease pathology and the development of biomaterials, more and more stimuli-responsive hydrogels will emerge to satisfy drug delivery and release ideal for the best therapeutic efficacy.

On the other hand, multiple stimuli-responsive drug-delivery hydrogels respond the complex of conditions in lesion area and favor the programming of drug liberation, but also create more expense and hardness to increase synthetic yield and product biocompatibility. Another big challenge is to design an appropriate program for the orderly occurrence of the established responsiveness, and it may be possible to see that these reactivities are not triggered in a right subsequence as programmed and thus fail to precisely tune drug delivery spatiotemporally. Additionally, no matter how well the stimuli-responsiveness of biomedical hydrogel works in preclinical studies, their real performances are demanded to be evaluated in human where the on/off switch of drug release is interfered by more complicated stimulatory factors that are impossible to be well reproduced with the xenografted tumors in experimental animals.

Finally, despite a good potential to govern drug delivery, most current stimuli-responsive injectable hydrogels still have to overcome drug burst, the small loading and excessive release of hydrophobic therapeutic agents, and the challenge to prolong the drug release in a demanded manner.[12] Recently, alginate hydrogels and PLGA (poly(D,L-lactic-*co*-glycolic acid) microspheres were combined to eliminate their respective flaws, such as quick clearance of microspheres by phagocytes and drug burst in gels,[143] displaying a promising combination delivery system for the future direction of local treatment.

Acknowledgements

This work was supported by National Natural Science Foundation of China (No. 81371675).

Conflict of Interest

The authors declare no conflict of interest.

Keywords

drug delivery, injectable hydrogels, stimuli responsiveness

Received: January 4, 2022
Revised: February 21, 2022
Published online: April 10, 2022

[1] Y. Yang, X. Liu, Y. Li, Y. Wang, C. Bao, Y. Chen, Q. Lin, L. Zhu, *Acta Biomater.* **2017**, *62*, 199.
[2] Y. N. Sun, D. Nan, H. Q. Jin, X. Z. Qu, *Polym. Test.* **2020**, *81*, 106283.
[3] A. Mandal, J. R. Clegg, A. C. Anselmo, S. Mitragotri, *Bioeng. Transl. Med.* **2020**, *5*, e10158.
[4] C.-W. P. Yun-Seok Rhee, P. P. DeLuca, H. M. Mansour, *Pharm. Technol.* **2010**, s6.
[5] A. Ali, S. Ahmed, *Int. J. Biol. Macromol.* **2018**, *109*, 273.
[6] N. Bhattarai, J. Gunn, M. Zhang, *Adv. Drug Delivery Rev.* **2010**, *62*, 83.
[7] R. Madonna, L. W. Van Laake, H. E. Botker, S. M. Davidson, R. De Caterina, F. B. Engel, T. Eschenhagen, F. Fernandez-Aviles, D. J. Hausenloy, J. S. Hulot, S. Lecour, J. Leor, P. Menasche, M. Pesce, C. Perrino, F. Prunier, S. Van Linthout, K. Ytrehus, W. H. Zimmermann, P. Ferdinandy, J. P. G. Sluijter, *Cardiovasc. Res.* **2019**, *115*, 488.
[8] Z. Y. Zhao, Z. Wang, G. Li, Z. W. Cai, J. Z. Wu, L. Wang, L. F. Deng, M. Cai, W. G. Cui, *Adv. Funct. Mater.* **2021**, *31*, 2103339.
[9] T. Garg, A. K. Goyal, *Expert Opin. Drug Delivery* **2014**, *11*, 767.
[10] S. Zhou, L. Li, C. Chen, Y. Chen, L. Zhou, F. H. Zhou, J. Dong, L. Wang, *Int. J. Med. Sci.* **2021**, *18*, 1910.

 © 2022 Wiley-VCH GmbH

[11] D. F. Emerich, S. R. Winn, P. Snodgrass, D. LaFreniere, M. Agostino, T. Wiens, H. Xiong, R. T. Bartus, *Pharm. Res.* **2000**, *17*, 776.
[12] F. Rizzo, N. S. Kehr, *Adv. Healthcare Mater.* **2021**, *10*, 2001341.
[13] A. A. Chaudhari, K. Vig, D. R. Baganizi, R. Sahu, S. Dixit, V. Dennis, S. R. Singh, S. R. Pillai, *Int. J. Mol. Sci.* **2016**, *17*, 1974.
[14] C. Mo, L. Xiang, Y. Chen, *Macromol. Rapid Commun.* **2021**, *42*, 2100025.
[15] D. Caccavo, S. Cascone, G. Lamberti, A. A. Barba, *Int. J. Pharm.* **2015**, *486*, 144.
[16] S. W. Kim, Y. H. Bae, T. Okano, *Pharm. Res.* **1992**, *9*, 283.
[17] C. C. Lin, A. T. Metters, *Adv. Drug Delivery Rev.* **2006**, *58*, 1379.
[18] T. Garg, S. Singh, A. K. Goyal, *Crit. Rev. Ther. Drug Carrier Syst.* **2013**, *30*, 369.
[19] S. L. Percival, S. McCarty, J. A. Hunt, E. J. Woods, *Wound Repair Regener.* **2014**, *22*, 174.
[20] A. Bansal, M. C. Simon, *J. Cell Biol.* **2018**, *217*, 2291.
[21] J. N. Moloney, T. G. Cotter, *Semin. Cell Dev. Biol.* **2018**, *80*, 50.
[22] E. M. Wilson, S. L. Moainie, J. M. Baskin, A. S. Lowry, A. M. Deschamps, R. Mukherjee, T. S. Guy, M. G. St John-Sutton, J. H. Gorman, 3rd, L. H. Edmunds, Jr., R. C. Gorman, F. G. Spinale, *Circulation* **2003**, *107*, 2857.
[23] A. Ceriello, *Diabetes Care* **2020**, *43*, 1169.
[24] C. Ding, L. Tong, J. Feng, J. Fu, *Molecules* **2016**, *21*, 1715.
[25] T. H. Tran, B. J. Lee, *Ther. Delivery* **2011**, *2*, 1199.
[26] K. T. Campbell, K. Wysoczynski, D. J. Hadley, E. A. Silva, *ACS Biomater. Sci. Eng.* **2020**, *6*, 308.
[27] L. Hovgaard, H. Brøndsted, *J. Controlled Release* **1995**, *36*, 159.
[28] M. T. Haseeb, M. A. Hussain, S. H. Yuk, S. Bashir, M. Nauman, *Carbohydr. Polym.* **2016**, *136*, 750.
[29] S. Vervoort, *Eng. Sci.* **2006**.
[30] H. Hezaveh, Muhamad, II, I. Noshadi, L. Shu Fen, N. Ngadi, *J. Microencapsulation* **2012**, *29*, 368.
[31] K. H. Bae, L.-S. Wang, M. Kurisawa, *J. Mater. Chem. B* **2013**, *1*, 5371.
[32] C. Hiemstra, L. J. van der Aa, Z. Zhong, P. J. Dijkstra, J. Feijen, *Macromolecules* **2007**, *40*, 1165.
[33] J. Qu, X. Zhao, P. X. Ma, B. Guo, *Acta Biomater.* **2017**, *58*, 168.
[34] X. Wang, C. Wang, Q. Zhang, Y. Cheng, *Chem. Commun.* **2016**, *52*, 978.
[35] F. Yang, J. Wang, L. Cao, R. Chen, L. Tang, C. Liu, *J. Mater. Chem. B* **2014**, *2*, 295.
[36] Y. Liang, Z. Li, Y. Huang, R. Yu, B. Guo, *ACS Nano* **2021**, *15*, 7078.
[37] M. C. Koetting, J. T. Peters, S. D. Steichen, N. A. Peppas, *Mater. Sci. Eng. R. Rep.* **2015**, *93*, 1.
[38] Y. Qiu, K. Park, *Adv. Drug Deliv. Rev.* **2001**, *53*, 321.
[39] S. Omidi, M. Pirhayati, A. Kakanejadifard, *Carbohydr. Polym.* **2020**, *231*, 115745
[40] X. Ma, T. Xu, W. Chen, H. Qin, B. Chi, Z. Ye, *Carbohydr. Polym.* **2018**, *179*, 100.
[41] Y. L. Chiu, S. C. Chen, C. J. Su, C. W. Hsiao, Y. M. Chen, H. L. Chen, H. W. Sung, *Biomaterials* **2009**, *30*, 4877.
[42] M. Pandey, N. Mohamad, M. C. Amin, *Mol. Pharmaceutics* **2014**, *11*, 3596.
[43] X. C. Fan, T. Wang, W. K. Miao, *J. Polym. Res.* **2018**, *25*, 215.
[44] Q. Zhang, L. Zhang, P. Wang, S. Du, *J. Pharm. Sci.* **2014**, *103*, 643.
[45] W. Qin, S. Long, M. Panunzio, S. Biondi, *Molecules* **2013**, *18*, 12264.
[46] A. Hameed, M. al-Rashida, M. Uroos, S. Abid Ali, K. M. Khan, *Expert Opin. Ther. Pat.* **2016**, *27*, 63.
[47] H. Yu, Y. Liu, H. Yang, K. Peng, X. Zhang, *Macromol. Rapid Commun.* **2016**, *37*, 1723.
[48] S. Guan, Y. Li, C. Cheng, X. Gao, X. Gu, X. Han, H. Ye, *Int. J. Biol. Macromol.* **2020**, *164*, 2418.
[49] R. Nguyen, I. Huc, *Chem. Commun.* **2003**, *8*, 942.
[50] F. Z. Kocak, A. C. S. Talari, M. Yar, I. U. Rehman, *Int. J. Mol. Sci.* **2020**, *21*, 1633.
[51] D. P. Huynh, G. J. Im, S. Y. Chae, K. C. Lee, D. S. Lee, *J. Controlled Release* **2009**, *137*, 20.
[52] D. P. Huynh, M. K. Nguyen, B. S. Pi, M. S. Kim, S. Y. Chae, K. C. Lee, B. S. Kim, S. W. Kim, D. S. Lee, *Biomaterials* **2008**, *29*, 2527.
[53] C. T. Huynh, M. K. Nguyen, D. P. Huynh, S. W. Kim, D. S. Lee, *Polymer* **2010**, *51*, 3843.
[54] C. T. Huynh, Q. V. Nguyen, S. W. Kang, D. S. Lee, *Polymer* **2012**, *53*, 4069.
[55] R. V. Kulkarni, R. Boppana, G. Krishna Mohan, S. Mutalik, N. V. Kalyane, *J. Colloid Interface Sci.* **2012**, *367*, 509.
[56] J. C. Garbern, E. Minami, P. S. Stayton, C. E. Murry, *Biomaterials* **2011**, *32*, 2407.
[57] S. Yu, X. Zhang, G. Tan, L. Tian, D. Liu, Y. Liu, X. Yang, W. Pan, *Carbohydr. Polym.* **2017**, *155*, 208.
[58] N. E. Kurland, R. B. Ragland, A. Zhang, M. E. Moustafa, S. C. Kundu, V. K. Yadavalli, *Int. J. Biol. Macromol.* **2014**, *70*, 565.
[59] X. Ding, Y. Wang, *J. Mater. Chem. B* **2017**, *5*, 887.
[60] S. Samimi Gharaie, S. M. H. Dabiri, M. Akbari, *Polymers* **2018**, *10*, 1317.
[61] Q. Tang, D. Zhao, Q. Zhou, H. Yang, K. Peng, X. Zhang, *Macromol. Rapid Commun.* **2018**, *39*, 1800109.
[62] J. Qu, X. Zhao, Y. Liang, T. Zhang, P. X. Ma, B. Guo, *Biomaterials* **2018**, *183*, 185.
[63] L. Zhao, L. Zhu, F. Liu, C. Liu, D. Shan, Q. Wang, C. Zhang, J. Li, J. Liu, X. Qu, Z. Yang, *Int. J. Pharm.* **2011**, *410*, 83.
[64] X. Wu, C. He, Y. Wu, X. Chen, *Biomater.* **2016**, *75*, 148.
[65] C. Lu, X. Wang, G. Wu, J. Wang, Y. Wang, H. Gao, J. Ma, *J. Biomed. Mater. Res. A* **2014**, *102*, 628.
[66] B. Bingol, S. Altuncu, F. D. Duman, A. Ak, U. Gulyuz, H. Y. Acar, O. Okay, D. Avci, *ACS Appl. Polym. Mater.* **2019**, *1*, 1724.
[67] V. H. Phan, T. Thambi, H. T. Duong, D. S. Lee, *Sci. Rep.* **2016**, *6*, 29978.
[68] T. M. D. Le, H. T. T. Duong, T. Thambi, V. H. Giang Phan, J. H. Jeong, D. S. Lee, *Biomacromolecules* **2018**, *19*, 3536.
[69] J. C. Garbern, A. S. Hoffman, P. S. Stayton, *Biomacromolecules* **2010**, *11*, 1833.
[70] Q. Gao, C. Zhang, M. Wang, Y. Wu, C. Gao, P. Zhu, *Polymer* **2020**, *197*, 122489.
[71] M. Ma, Y. Zhong, X. Jiang, *Carbohydr. Polym.* **2020**, *236*, 116096.
[72] J. Shi, W. Guobao, H. Chen, W. Zhong, X. Qiu, M. M. Q. Xing, *Polym. Chem.* **2014**, *5*, 6180.
[73] H. Wang, S. C. Heilshorn, *Adv. Mater.* **2015**, *27*, 3717.
[74] C. D. Meyer, C. S. Joiner, J. F. Stoddart, *Chem. Soc. Rev.* **2007**, *36*, 1705.
[75] Z. Q. Lei, P. Xie, M. Z. Rong, M. Q. Zhang, *J. Mater. Chem. A* **2015**, *3*, 19662.
[76] A. Andersen, M. Krogsgaard, H. Birkedal, *Biomacromolecules* **2018**, *19*, 1402.
[77] L. Wang, Y. Li, L. Lin, R. Mu, J. Pang, *Carbohydr. Polym.* **2020**, *236*, 116045.
[78] M. Rizwan, R. Yahya, A. Hassan, M. Yar, A. D. Azzahari, V. Selvanathan, F. Sonsudin, C. N. Abouloula, *Polymers* **2017**, *9*, 137.
[79] M. L. Pua, T. Yoshitomi, P. Chonpathompikunlert, A. Hirayama, Y. Nagasaki, *J. Controlled Release* **2013**, *172*, 914.
[80] Z. Zhang, J. Wan, L. Sun, Y. Li, J. Guo, C. Wang, *J. Controlled Release* **2016**, *225*, 96.
[81] B. Sun, C. Luo, H. Yu, X. Zhang, Q. Chen, W. Yang, M. Wang, Q. Kan, H. Zhang, Y. Wang, Z. He, J. Sun, *Nano Lett.* **2018**, *18*, 3643.
[82] W. Wang, J. Chen, M. Li, H. Jia, X. Han, J. Zhang, Y. Zou, B. Tan, W. Liang, Y. Shang, Q. Xu, S. A, W. Wang, J. Mao, X. Gao, G. Fan, W. Liu, *ACS Appl. Mater. Interfaces* **2019**, *11*, 2880.
[83] X. Cheng, Y. Jin, T. Sun, R. Qi, H. Li, W. Fan, *Colloids Surf. B* **2016**, *141*, 44.
[84] X. Xu, W. Lu, J. Zhu, X. Pan, X. Zhu, *Gels* **2021**, *7*, 21.

© 2022 Wiley-VCH GmbH

[85] W. Lu, X. Xu, L. Imbernon, J. Zhu, R. Hoogenboom, F. E. Du Prez, X. Pan, *Biomacromolecules* **2020**, *21*, 3308.
[86] C. Feng, D. Zhu, L. Chen, Y. Lu, J. Liu, N. Y. Kim, S. Liang, X. Zhang, Y. Lin, Y. Ma, C. Dong, *Front. Pharmacol.* **2019**, *10*, 369.
[87] L. Wang, W. Cao, Y. Yi, H. Xu, *Langmuir* **2014**, *30*, 5628.
[88] C. Gong, M. Shan, B. Li, G. Wu, *J. Biomed. Mater. Res. A* **2017**, *105*, 2451.
[89] H. J. Won, B. Ryplida, S. G. Kim, G. Lee, J. H. Ryu, S. Y. Park, *ACS Nano* **2020**, *14*, 8409.
[90] D. Lyu, S. Chen, W. Guo, *Small* **2018**, *14*, 1704039.
[91] L. D. Amer, S. J. Bryant, *Ann. Biomed. Eng.* **2016**, *44*, 1959.
[92] B. P. Purcell, D. Lobb, M. B. Charati, S. M. Dorsey, R. J. Wade, K. N. Zellars, H. Doviak, S. Pettaway, C. B. Logdon, J. A. Shuman, P. D. Freels, J. H. Gorman, 3rd, R. C. Gorman, F. G. Spinale, J. A. Burdick, *Nat. Mater.* **2014**, *13*, 653.
[93] N. Joshi, J. Yan, S. Levy, S. Bhagchandani, K. V. Slaughter, N. E. Sherman, J. Amirault, Y. Wang, L. Riegel, X. He, T. S. Rui, M. Valic, P. K. Vemula, O. R. Miranda, O. Levy, E. M. Gravallese, A. O. Aliprantis, J. Ermann, J. M. Karp, *Nat. Commun.* **2018**, *9*, 1275.
[94] Y. Kasahara, Y. Sato, M. K. Masukawa, Y. Okuda, M. Takinoue, *APL Bioeng.* **2020**, *4*, 016109.
[95] Y. He, X. Yang, R. Yuan, Y. Chai, *J. Mater. Chem. B* **2019**, *7*, 2643.
[96] J. Zhang, Y. Guo, G. Pan, P. Wang, Y. Li, X. Zhu, C. Zhang, *ACS Appl. Mater. Interfaces* **2020**, *12*, 21441.
[97] J. Chen, Y. Zhu, H. Liu, L. Wang, *Top. Curr. Chem.* **2020**, *378*, 32.
[98] N. Ahmad, M. C. Mohd Amin, I. Ismail, F. Buang, *Expert Opin. Drug Delivery* **2016**, *13*, 621.
[99] L. Zhao, L. Niu, H. Liang, H. Tan, C. Liu, F. Zhu, *ACS Appl. Mater. Interfaces* **2017**, *9*, 37563.
[100] F. Zhao, D. Wu, D. Yao, R. Guo, W. Wang, A. Dong, D. Kong, J. Zhang, *Acta Biomater.* **2017**, *64*, 334.
[101] W. L. Brooks, B. S. Sumerlin, *Chem. Rev.* **2016**, *116*, 1375.
[102] X. Li, M. Fu, J. Wu, C. Zhang, X. Deng, A. Dhinakar, W. Huang, H. Qian, L. Ge, *Acta Biomater.* **2017**, *51*, 294.
[103] H. Kim, H. Lee, K. Y. Seong, E. Lee, S. Y. Yang, J. Yoon, *Adv. Healthcare Mater.* **2015**, *4*, 2071.
[104] D. Chen, C. Chen, C. Huang, T. Chen, Z. Liu, *Front. Chem.* **2020**, *8*, 251.
[105] X. Zhu, H. Zhang, H. Huang, Y. Zhang, L. Hou, Z. Zhang, *Nanotechnology* **2015**, *26*, 365103.
[106] H. Zhang, X. Zhu, Y. Ji, X. Jiao, Q. Chen, L. Hou, H. Zhang, Z. Zhang, *J. Mater. Chem. B* **2015**, *3*, 6310.
[107] G. Yang, X. Wan, Z. Gu, X. Zeng, J. Tang, *J. Mater. Chem. B* **2018**, *6*, 1622.
[108] Y. Yang, W. Zhu, Z. Dong, Y. Chao, L. Xu, M. Chen, Z. Liu, *Adv. Mater.* **2017**, *29*.
[109] L. Grealish, A. Lomasney, B. Whiteman, *Cancer Nurs.* **2000**, *23*, 237.
[110] C. Liu, X. Guo, C. Ruan, H. Hu, B. P. Jiang, H. Liang, X. C. Shen, *Acta Biomater.* **2019**, *96*, 281.
[111] S. Tamesue, Y. Takashima, H. Yamaguchi, S. Shinkai, A. Harada, *Angew. Chem. Int. Ed. Engl.* **2010**, *49*, 7461.
[112] C. A. DeForest, K. S. Anseth, *Angew. Chem. Int. Ed.* **2012**, *51*, 1816.
[113] Y. Cheng, C. He, K. Ren, Y. Rong, C. Xiao, J. Ding, X. Zhuang, X. Chen, *Macromol. Rapid Commun.* **2018**, *39*, 1800272.
[114] X. Xu, Z. Zeng, Z. Huang, Y. Sun, Y. Huang, J. Chen, J. Ye, H. Yang, C. Yang, C. Zhao, *Carbohydr. Polym.* **2020**, *229*, 115394.
[115] W. Shi, J. Huang, R. Fang, M. Liu, *ACS Appl. Mater. Interfaces* **2020**, *12*, 5177.
[116] M. Moros, J. Idiago-Lopez, L. Asin, E. Moreno-Antolin, L. Beola, V. Grazu, R. M. Fratila, L. Gutierrez, J. M. de la Fuente, *Adv. Drug Delivery Rev.* **2019**, *138*, 326.
[117] J. Zeng, D. Shi, Y. Gu, T. Kaneko, L. Zhang, H. Zhang, D. Kaneko, M. Chen, *Biomacromolecules* **2019**, *20*, 3375.
[118] J. Qin, I. Asempah, S. Laurent, A. Fornara, R. N. Muller, M. Muhammed, *Adv. Mater.* **2009**, *21*, 1354.
[119] H. Wu, L. Song, L. Chen, W. Zhang, Y. Chen, F. Zang, H. Chen, M. Ma, N. Gu, Y. Zhang, *Acta Biomater.* **2018**, *74*, 302.
[120] S. M. N. Simões, A. Rey-Rico, A. Concheiro, C. Alvarez-Lorenzo, *Chem. Commun.* **2015**, *51*, 6275.
[121] Z. Chen, C. Yan, S. Yan, Q. Liu, M. Hou, Y. Xu, R. Guo, *Theranostics* **2018**, *8*, 1146.
[122] X. Liu, A. L. Miller, 2nd, S. Park, B. E. Waletzki, Z. Zhou, A. Terzic, L. Lu, *ACS Appl. Mater. Interfaces* **2017**, *9*, 14677.
[123] S. Martino, F. D'Angelo, I. Armentano, J. M. Kenny, A. Orlacchio, *Biotechnol. Adv.* **2012**, *30*, 338.
[124] W. Wang, B. Tan, J. Chen, R. Bao, X. Zhang, S. Liang, Y. Shang, W. Liang, Y. Cui, G. Fan, H. Jia, W. Liu, *Biomaterials* **2018**, *160*, 69.
[125] S. A. Makohliso, R. F. Valentini, P. Aebischer, *J. Biomed. Mater. Res.* **1993**, *27*, 1075.
[126] J. Xu, Y. L. Tsai, S. H. Hsu, *Molecules* **2020**, *25*, 5296.
[127] F. Huang, T. Chen, J. Chang, C. Zhang, F. Liao, L. Wu, W. Wang, Z. Yin, *Int. J. Biol. Macromol.* **2021**, *167*, 434.
[128] Q. Rong, W. Lei, M. Liu, *Chemistry* **2018**, *24*, 16930.
[129] R. Balint, N. J. Cassidy, S. H. Cartmell, *Acta Biomater.* **2014**, *10*, 2341.
[130] L. Dai, *J. Macromol. Sci., Part C: Polym. Rev.* **1999**, *39*, 273.
[131] V. Pillay, T. S. Tsai, Y. E. Choonara, L. C. du Toit, P. Kumar, G. Modi, D. Naidoo, L. K. Tomar, C. Tyagi, V. M. Ndesendo, *J. Biomed. Mater. Res. Part A* **2014**, *102*, 2039.
[132] J. Qu, X. Zhao, P. X. Ma, B. Guo, *Acta Biomater.* **2018**, *72*, 55.
[133] C. Marquez-Chin, M. R. Popovic, *Biomed. Eng. Online* **2020**, *19*, 34.
[134] G. A. Husseini, W. G. Pitt, *Adv. Drug Delivery Rev.* **2008**, *60*, 1137.
[135] W. C. Huang, F. Ali, J. Zhao, K. Rhee, C. Mou, C. J. Bettinger, *Biomacromolecules* **2017**, *18*, 1162.
[136] F. Z. Yuan, H. F. Wang, J. Guan, J. N. Fu, M. Yang, J. Y. Zhang, Y. R. Chen, X. Wang, J. K. Yu, *Pharmaceutics* **2021**, *13*, 1487.
[137] C. H. Wu, M. K. Sun, Y. Kung, Y. C. Wang, S. L. Chen, H. H. Shen, W. S. Chen, T. H. Young, *Ultrason. Sonochem.* **2020**, *62*, 104875.
[138] N. Huebsch, C. J. Kearney, X. Zhao, J. Kim, C. A. Cezar, Z. Suo, D. J. Mooney, *Proc. Natl. Acad. Sci. U. S. A.* **2014**, *111*, 9762.
[139] S. Mura, J. Nicolas, P. Couvreur, *Nat. Mater.* **2013**, *12*, 991.
[140] X. Xu, Z. Huang, Z. Huang, X. Zhang, S. He, X. Sun, Y. Shen, M. Yan, C. Zhao, *ACS Appl. Mater. Interfaces* **2017**, *9*, 20361.
[141] J. Park, S. Pramanick, D. Park, J. Yeo, J. Lee, H. Lee, W. J. Kim, *Adv. Mater.* **2017**, *29*.
[142] J. Xiong, R. Xie, H. Zhang, J. Gao, J. Wang, Q. Liang, *J. Hazard. Mater.* **2021**, *411*, 125150.
[143] J. Lee, M. J. Cha, K. S. Lim, J. K. Kim, S. K. Lee, Y. H. Kim, K. C. Hwang, K. Y. Lee, *J. Drug Targeting* **2013**, *21*, 822.

© 2022 Wiley-VCH GmbH



Chunxiang Mo received her bachelor's degree in pharmaceutical science from University of South China, Hengyang, China in 2019. She is currently pursuing her master's degree under Dr. Yuping Chen's supervision. Her research interest is the responsive injectable hydrogels in biomedical therapy.



Rui Luo obtained her bachelor's degree in pharmacy from Shaoyang University in June 2021. As a graduate student in Dr. Yuping Chen's research team, she is working on injectable hydrogels for tissue engineering applications.



Yuping Chen is currently a full professor in the School of Pharmacy at the University of South China. She obtained her Ph.D. in 2000 from the Chinese Academy of Medical Sciences and Peking Union Medical College, Beijing, China. Her research is to discover new molecular targets and drugs and to develop novel therapeutic delivery systems.

© 2022 Wiley-VCH GmbH